CHAPTER 19

Fluid Mixing Technology in the Petroleum Industry

RAMESH R. HEMRAJANI

ExxonMobil Research and Engineering Company

19-1 INTRODUCTION

Mixing applications in petroleum industry may be somewhat limited compared to chemical, pharmaceutical, and food manufacturing. In addition, refinery streams are less complex then specialty and fine chemicals in terms of fluid physical properties and process conditions. However, due to large volumes of petroleum streams to be mixed, mixing technology plays an important role in enhancing productivity and profitability. Of course, the petroleum companies that have large integrated chemicals operations use most aspects of mixing technology in reacting and nonreacting single- and multiphase systems. The refining processes involving mixing operations include making emulsion products for oil drilling, absorption of CO_2 from natural gas, crude oil–water homogenization for custody transfer, sludge suspension in crude oil storage tanks, desalting of crude oil, alkylation, caustic–oil contacting for neutralization, pH control, and more. Small enhancements in mixing efficiency can yield large benefits in reduced investment and operating costs.

A typical refinery flow scheme is described in Figure 19-1. Crude oil produced at onshore and offshore drilling fields is transported via pipelines and/or ships to the refineries. It is then stored in large (up to 1 Mbbl) tanks for several days. Sometimes a terminal with several large storage tanks is involved for temporary storage of crude oils and/or blending before pumping to refineries. The first step in crude processing consists of removing salt by emulsifying water and then demulsifying in an electrostatic field. Chemical aids are sometimes mixed in to improve water emulsification and demulsification. The oil is then processed in

Handbook of Industrial Mixing: Science and Practice, Edited by Edward L. Paul, Victor A. Atiemo-Obeng, and Suzanne M. Kresta
ISBN 0-471-26919-0

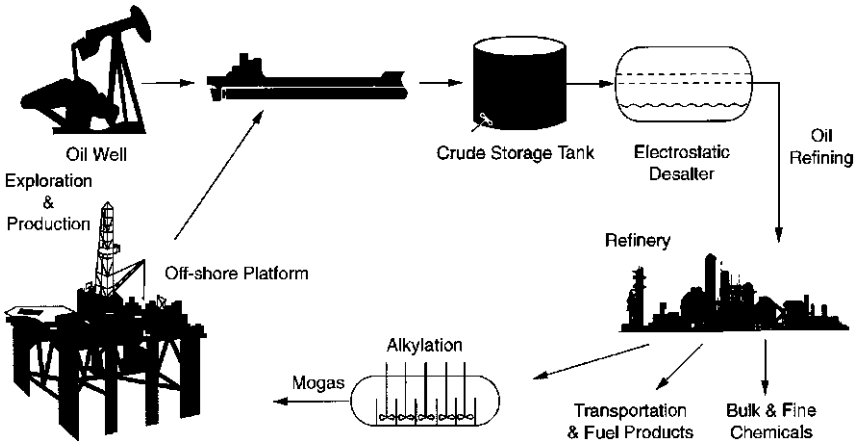

Figure 19-1 Typical petroleum operations.

the refinery to make transportation/fuel products and feedstocks for bulk and fine chemicals. Part of the product stream is used to produce an alkylate by acid catalysis in mixing tanks. This alkylate is blended into the gasoline to increase its octane number.

Mixing plays important roles in many processing steps in the refinery's upstream and downstream areas listed below. The role of mixing technology in chemical operations is not discussed in this chapter, but it is covered in other chapters on single and multiphase systems.

Mixing in upstream operations

- Control fluid for oil drilling wells
- Gas treating on onshore and offshore platforms
- Oil/water homogenization in transfer lines

Mixing in downstream operations

- Sludge control in crude oil storage tanks
- Crude oil blending
- In-line mixing of water for desalting
- Solids suspension in bottoms slurry tanks
- Fuels and products blending tanks
- Acid/hydrocarbon mixing for alkylation
- Caustic/oil and water/oil contacting
- Acid or caustic mixing for pH control in wastewater treatment
- Caustic/gasoline emulsification for converting elemental sulfur

19-2 SHEAR-THICKENING FLUID FOR OIL DRILLING WELLS

Fluids with unique thickening properties are used during blowout and lost circulation of oil drilling wells. When pumped into pores surrounding the well, this fluid hardens and plugs the pores. The thickening time is required to be longer than 50 min to avoid premature stoppage of the flow. This fluid consists of a mixture of clay and a stabilized water-in-oil emulsion. The emulsion is prepared batchwise by dispersing water in oil in agitated tanks. Since this mixture is kept available nearby drilling wells, it must be highly stable to prevent settling out during long storage. The stability of the emulsion is achieved by forming a solid protective film at the interface between the water droplets and the continuous oil phase. The protective film is a product of a reaction between polyisobutylene succinic acid (PIBSA) and polyacrylic acid (Figure 19-2). These chemicals are added into the oil and water phases, respectively, before emulsification. During the mixing operation, the two reactants diffuse to the interface, where they react to form a stabilizing solid coating around the drops.

The mixing issues in designing a suitable mixing system for the manufacture of this shear-thickening emulsion are:

- Three volumes of water must be dispersed in one volume of oil, creating a potential for undesired phase inversion. Therefore, water must be added to the oil slowly with the mixer on.
- A narrow drop size distribution of the emulsion is desired for best shear thickening properties. The impeller selection, therefore, should be based on providing narrow distribution of shear.
- Formation of a thin protective coating around the dispersed drops is needed for emulsion to be stable. The emulsion stability is necessary for long shelf life at the oil field.

A laboratory study in two different-sized mixing tanks equipped with single pitched blade turbines lead to the following correlation for maximum drop size

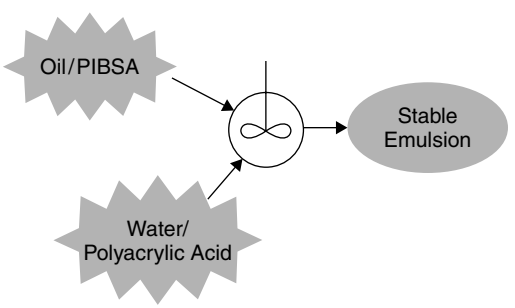

Figure 19-2 Mixing of two phases to form a stable emulsion.

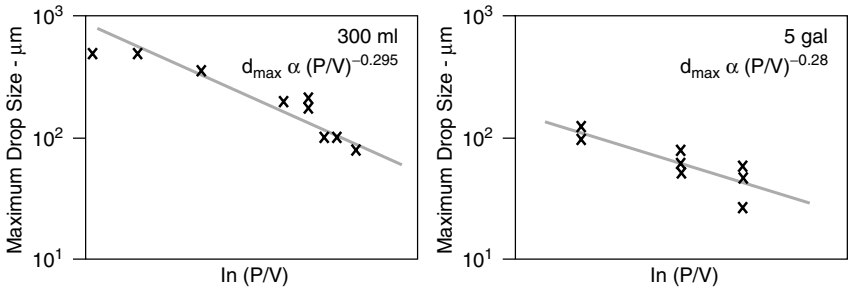

Figure 19-3 Maximum drop size as a function of P/V: pitched blade turbine.

d_{max} with mixing energy as power per unit volume P/V (Figure 19-3).

$$d_{max} = \left(\frac{P}{V}\right)^{-0.3}$$

The product analyses from these experiments indicated that the desired shear thickening properties are best achievable with maximum drop size of about 600 μm. A suitable mixing system consisting of a pitched blade turbine scaled up on the basis of constant power per unit volume has been commercially successful. Further improvements can be achieved by producing narrower distribution of drop sizes, perhaps through using hydrofoil impellers. The experiments with radial flow impellers yielded inferior product quality.

19-3 GAS TREATING FOR CO_2 REDUCTION

Natural gas often contains a high concentration (>2%) of CO_2, which makes it unsuitable for direct use as fuel gas. Conventional process for reducing this concentration to below 2% consists of absorption of CO_2 in an amine solution. The amine solution is regenerated and recycled back into the process. The absorption is carried out at pressures in excess of 100 bar and with a gas/liquid volumetric ratio of about 2 : 1. Packed bed contactors operated in countercurrent mode are commonly used for this purpose. Although these towers provide maximum driving force for mass transfer, they can be bulky and heavy with dimensions 5 m diameter by 25 m high, depending on the feed rates. They are, therefore, less suitable for use on offshore platforms. Static mixers can be the favored choice because of the following advantages:

- Plug flow conditions are available with
  - a large number of stages
  - good radial mixing
  - negligible axial mixing

- High mass transfer coefficient ($k_g a$ can be 10 to 20 times higher than in packed towers)
- Target product CO_2 concentration achievable in short residence time (1 or 2 s)
- Smaller in size and weight, with ease of installation on floating platforms
- Can be horizontal, vertical, or inclined (horizontal and inclined need to be within certain boundary conditions for successful application)
- Can easily handle foaming systems

Design guidelines for static mixers for this application are not available in the literature and therefore need to be developed through experimentation. Fundamental concepts of gas–liquid contacting in static mixers, discussed in Chapter 7, can be used to select an appropriate mixer type. Since no literature data are available for the specific fluids at process conditions, it is advised to conduct pilot plant tests at scale at actual pressures to quantify the effect of mixer pressure drop on mass transfer rate and to develop scale-up criteria.

19-4 HOMOGENIZATION OF WATER IN CRUDE OIL TRANSFER LINES

When crude oil is sampled for determination of water content, as a part of custody transfer, it is essential that the water be uniformly dispersed across the pipe cross-section. In the absence of good mixing, water can get stratified and flow near the pipe bottom and escape the sampler. While adequate mixing must be provided to create good dispersion; the resulting emulsion should not be stable, because water must later settle easily in storage tanks. Typical sizes of pipelines used for transferring oil range from 12 to 30 in. in diameter. The selection and design of an effective mixing system requires careful evaluation of various technologies for minimizing investment costs. Optimum mixing can add a high value for the refiner, as the cost of 0.1% sampling error can amount to $250 000 per medium-sized tanker.

The mixing system for adequate homogenization of water should be capable of handling changing flow rate because the ship pumps often operate at varying rates. The type and design of such a mixer depends on the length of the pipe, upflow/downflow sections, and pressure drop, creating elements such as bends and valves. The pipeline velocity requirements for adequate dispersion with different mixers and pipeline configurations can be obtained from the chart shown in Figure 19-4. This chart, based on field data, indicates that for less than 8 ft/s (2.5 m/s) oil velocity, some form of mixing is required. It can be used for deciding on the type of mixer needed based on oil velocity during normal and turndown rates.

When crude oil velocity is low and natural turbulence is inadequate even with pipe bends and valves, the following four types of mixers are commonly used:

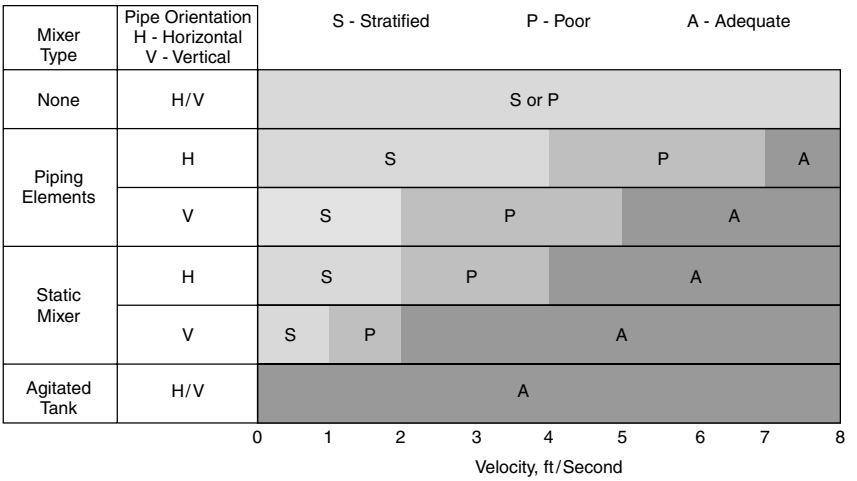

Figure 19-4 Pipeline velocity requirements with different mixers.

- Fixed geometry static mixers
- Variable geometry in-line mixers
- Rotary in-line blender
- Recirculating jet mixer

19-4.1 Fixed Geometry Static Mixers

The simplest type of fixed geometry in-line mixer is a distributor inside a pipe (Figure 19-5*a*), marketed by Neyrtec of France. This mixer is designed to create pressure drop in the two-phase flow through two perforated plates placed facing one another, and provide energy for dispersion. In addition, opposed jets are formed to create further shear, useful for breakup and homogenization of

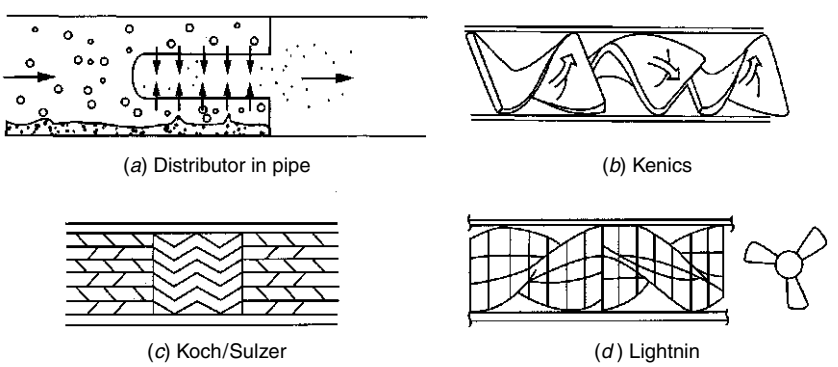

Figure 19-5 Fixed geometry in-line mixers.

dispersed drops. Total energy per unit mass, E_m, is given by

$$E_m = Q\frac{\Delta P}{\rho V}$$

where Q is the flow rate, ΔP the pressure drop, ρ the liquid density, and V the mixer volume.

The pressure drop, ΔP, can be either measured for a given design or estimated based on distributor open area and physical properties of the emulsion. In this type of mixer the energy dissipation can be on the order of 0.4 kW/kg. The maximum drop size of dispersion, d_{max}, is related to E_m by

$$d_{max} \propto E_m^{-0.4}\left(\frac{\rho}{\sigma}\right)^{-0.6}$$

where σ is the interfacial tension.

There are a number of static mixers that can be used for liquid–liquid dispersion. Three of them—Kenics (Fasano and Ryan, 1988), Koch/Sulzer, and Lightnin—are shown in Figure 19-5*b–d*. These static mixers are compact pipe internals designed to provide radial mixing and turbulence to cause dispersion and to homogenize the emulsion in the pipe. The internals consist of a sequence of vanes that force the flowing fluid to change direction abruptly several times, thus imposing large shear forces on the fluid. The energy spent is delivered by the pump on the ship or at a terminal, and therefore no power supply is needed at the mixer location.

Literature data on dispersion in static mixers indicate that the Sauter mean diameter of dispersed drops can be correlated with Weber number and friction factor by

$$\frac{d_{32}}{D} \propto We^{-0.6}f^{-0.4}$$

where d_{32} is the Sauter mean diameter, D the pipe diameter, We the Weber number ($= \rho v^2 D/\sigma$, where v is the velocity), and f is the friction factor.

If designed and operated at design pressure drop, these static mixers can produce a narrow drop size distribution. For example, 70% of dispersed volume can be within 20% of the mean drop diameter. However, these mixers work poorly at low velocities, because the pressure drop can fall below the necessary level. Also, at extremely high velocities, there is a danger of stable emulsion formation.

19-4.2 Variable Geometry In-line Mixer

The static mixer shown in Figure 19-6 overcomes the disadvantage of conventional static mixers by maintaining pressure drop and mixing energy constant over a wide range of flow rates. A servo system is used to vary the area of apertures as the flow rate varies. Creating opposing jets and turbulence in the mixer volume carries out mixing of dispersed aqueous drops. Although this mixer is

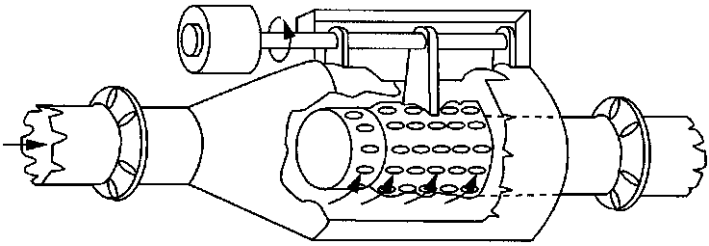

Figure 19-6 Example of a variable geometry in-line mixer.

highly suitable for homogenization of water-in-oil in a wide range of flow rates, it is bulky and expensive.

19-4.3 Rotary In-line Blender

When crude oil velocity in large pipes is expected to be low, the small mixing tanks shown in Figure 19-7 are installed just upstream of the sampler. The design consists of at least two stages, each with an impeller, and internal baffles. The incoming flow is forced to pass through each stage with strategically designed baffles before exiting. The impellers can be radial flow or axial flow, and the mixer is sized to provide power per unit volume in the range 5 to 20 hp/kgal. This blender is installed in an oversized section of the pipe in order to increase residence time and reduce superficial velocity. More than two stages can be used to provide narrower residence time distribution. This mixer works best at low flow rates when mixing is most needed. When the flow rate is high, the mixer

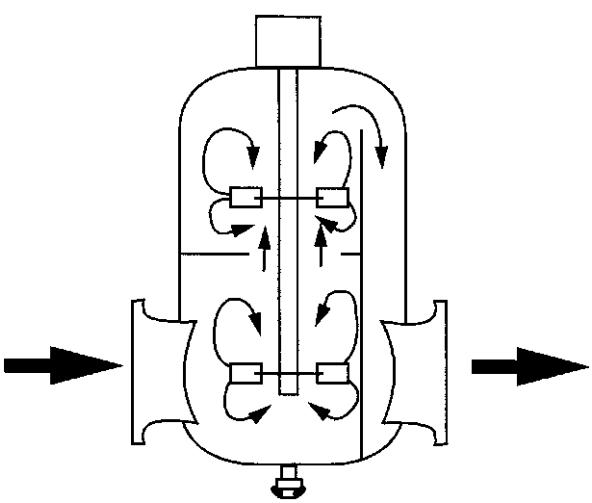

Figure 19-7 Rotary in-line blender.

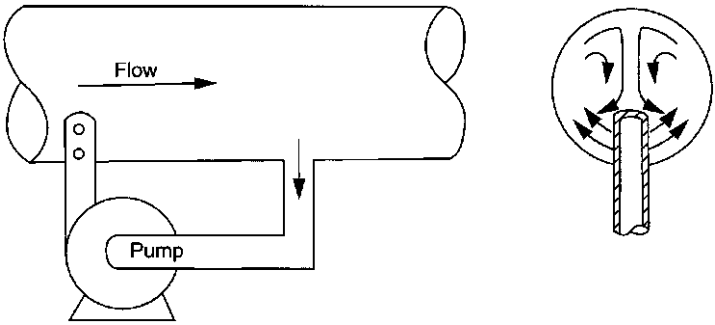

Figure 19-8 Recirculating jet mixer.

can be turned off to prevent formation of a stable emulsion. It takes a significant head loss, however, and requires power supply at remote locations.

19-4.4 Recirculating Jet Mixer

The mixer shown in Figure 19-8 consists of a bypass loop with a pump to recirculate a portion of the flowing liquid, and reinject under pressures a series of jets which dissipate their energy through turbulent mixing with the main flow. In addition, these jets induce large scale vortices important for homogenization of dispersed drops. The jet nozzles, manufactured by Jiskoot, Inc. of Houston, are designed to provide velocities in the range 20 to 25 ft/s (6.5 to 8.3 m/s). Instead of generalized turbulence and shear in the whole fluid mass, the jet energy is concentrated locally near the bottom, where water concentration is expected to be highest. These jets are effective in dispersing settled water drops and evenly distributing over the complete cross-section of the pipe by twin helix rotation. The pump is generally sized at 7 bar above the line pressure, and its suction can be either downstream or upstream of the jets. The jet velocity can be varied independent of the pipe flow rate. Other than the jet nozzle, there are no protruding metal parts, and therefore the pressure loss is minimal. The pump is installed externally and can easily be repaired or replaced. When there is adequate velocity for mixing, the pump can be turned off to reduce additional energy input. The only disadvantage is that a power supply for the pump must be provided at remote locations.

19-5 SLUDGE CONTROL IN CRUDE OIL STORAGE TANKS

Crude oil almost always carries with it some amount of bottom sludge and water (BS&W) at a typical concentration of about 0.5 wt %. Sludge comprises a mixture of organic and inorganic products with water in the form of both types of stable emulsions, oil-in-water and water-in-oil. These products include waxes, asphaltenes, polymers, organic acids, salt, mud, sand, and corrosion products.

Because sludge is heavier than crude oil, it settles in storage vessels at terminals and refineries.

Excessive sludge accumulation can occur in tanks equipped with underpowered and/or improperly operated mixers. Low ambient temperatures can also cause reduced sludge dispersion and hydrocarbon solubility. Occasionally, crude oil tankers clean their ship tanks and pump high concentrations of sludge to storage tanks. Heavier and high sulfur crude oils carry higher than 0.5 wt % sludge. Once settled on the tank floor, the sludge hardens and cannot be removed by normal pumping.

Sludge settled on the tank floor can cause several problems such as:

- Loss of storage capacity or incorrect capacity assumptions
- Entrapment of settled water, which can occasionally leave as slugs and create operating problems in the downstream equipment, e.g.,
  - desalter overload, increased water carryover, and oil carryunder
  - crude preheat train fouling
  - pressure buildup in the pipestill
- Safety and environmental problems such as:
  - landing of floating roof on an uneven sludge layer
  - potential tank boilover due to trapped water in the event of fire
- Frequent need for off-stream tank cleaning, which is hazardous, expensive, time consuming, and requires sludge disposal
- Corrosion of the wall

Adequate mixing is therefore important for preventing settling of sludge on the tank floor and for suspending sludge that has hardened due to long-term accumulation. Conventional mixing systems used for this application are:

- Side-entering mixers
- Rotating submerged jet nozzles

19-5.1 Side-Entering Mixers

Side-entering mixers consist of a marine propeller or a hydrofoil impeller attached to a horizontal shaft and installed on the tank shell near the bottom. This mixer type generates a horizontal spiraling jet that provides the desired thrust to dislodge and entrain the sludge. The mixer shaft is positioned at a fixed angle of about 10° to the left of the tank diameter when the mixer is rotating clockwise looking from the motor side. If the mixer is installed facing the tank center, a vortex can be formed, resulting in sludge buildup in the tank center. The mixers can be designed

Table 19-1 Guidelines for Selecting Number of Side Entering Mixers

Tank diameter (m)	<30	30–45	45–60	>60
Number of mixers	1	2	3	4 or 5

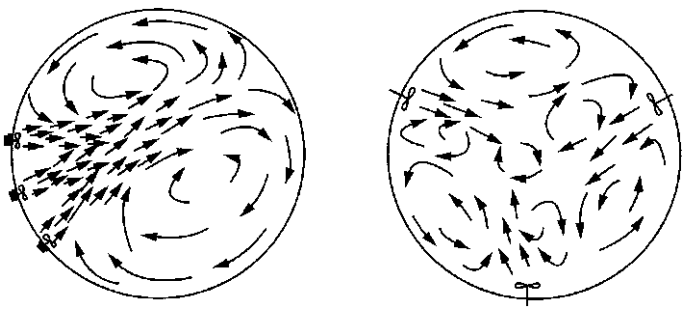

(*a*) (*b*)

Figure 19-9 Side-entering mixers.

with flexibility of changing angle from -30° to $+30^\circ$. These swivel angle mixers are more effective than a fixed-angle mixer for keeping the tank floor clean.

The mixer drives are generally limited to 60 hp for gear-driven and 100 hp for belt-driven systems, although larger mixers have occasionally been used. Since crude oil storage tanks can be very large, up to 300 ft in diameter, multiple mixers are commonly employed to provide adequate mixing energy. Guidelines for selecting appropriate number of mixers are given in Table 19-1. Multiple mixers generally are of equal size and can be installed in a clustered (Figure 19-9*a*) or distributed (Figure 19-9*b*) configuration. Field data indicate that the mixer performance with these two configurations are about the same if the total energy is adequate. It is recommended to install the tank outlet opposite the clustered mixers.

The side-entering mixers should be designed at a minimum of 0.4 hp/kbbl for light to medium crude oils. For heavy and high sludge containing crudes, higher mixing energy is needed to maintain sludge in suspension. This design guideline is based on sludge monitoring carried out for one year in two tanks equipped with mixers designed at 0.4 and 0.3 hp/kbbl. The data in Figure 19-10 clearly show that 0.4 hp/kbbl is required to minimize sludge accumulation. It should be noted that due to higher crude temperatures in summer months, the accumulated sludge volume is considerably reduced.

19-5.2 Rotating Submerged Jet Nozzle

A jet mixer can be designed to deliver a concentrated horizontal force on the tank floor to dislodge settled sludge. This jet must, however, be rotated to cover the entire floor. The jet can be energized by the oil flow during receipt or by pumping

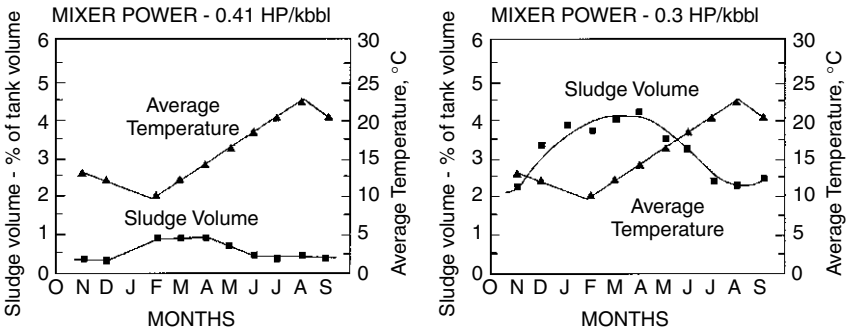

Figure 19-10 Sludge measurements in two crude oil tanks at different mixer power.

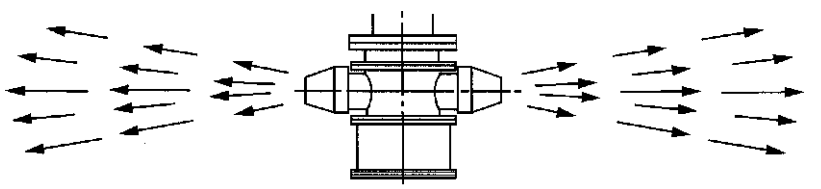

Figure 19-11 Rotating submerged jet nozzles: P43 machine.

around the oil in the tank. Although a single rotating jet can be operated, a mixer with two diametrically opposite nozzles can have a better balance of forces on the mixer body. The latter design is marketed as the P43 machine by Sarp UK Ltd. and shown in Figure 19-11.

The P43 machine design is based on the required cleaning radius R, oil pumping rate, and available pressure drop. A portion of the flow is directed to an impeller inside the machine, which through a series of gears rotates the nozzles at rates from 1.5 to 3.5 deg/min. The P43 installation can be center mounted (CM) or shell mounted (SM). The CM system is cost-effective because only one machine is needed. In addition, the cleaning distance is equal to the tank radius and requires a lower pumping rate than do the SM machines. However, the tank must be fully cleaned and degassed before installation. The SM system can be installed safely, with the crude oil level lowered to below the manhole. Therefore, this configuration is selected when initial desludging is required followed by continued sludge control. The cleaning radius R of the SM system depends on the number of P43 machines, as shown in Figure 19-12. These machines can be operated sequentially for 8 h each, since sludge settling rates are quite slow.

The required pumping rate and pressure drop for effective sludge suspension can be calculated from

$$Q = 7.56d^2 \left(\frac{R}{d}\right)^{1.01} \qquad \text{gal/min}$$

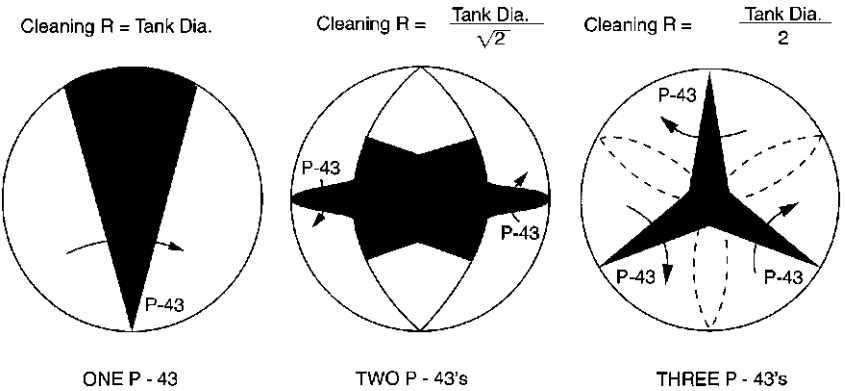

Figure 19-12 Shell-mounted P43 configurations.

$$\Delta P = S\left(\frac{Q}{26.82d^2}\right)^2 \qquad \text{psi}$$

where d is the nozzle diameter in inches, R the cleaning radius in feet, and S the specific gravity of the crude. Rotating submerged jet mixers are capable of both preventing sludge accumulation and suspending settled sludge, whereas side-entering mixers are only expected to prevent sludge settling. The guidelines discussed above are for normal crudes and not applicable to heavy crudes or slop oils.

19-6 DESALTING

Desalting is a process for removing salt from crude oil before sending it to the pipestill. This is done by first mixing a demulsifier in the pipe carrying crude oil, which is then followed by emulsifying fresh water using an in-line mixer (Figure 19-13). The water-in-oil emulsion is broken in an electrostatic separator to produce oil with negligible salt and water.

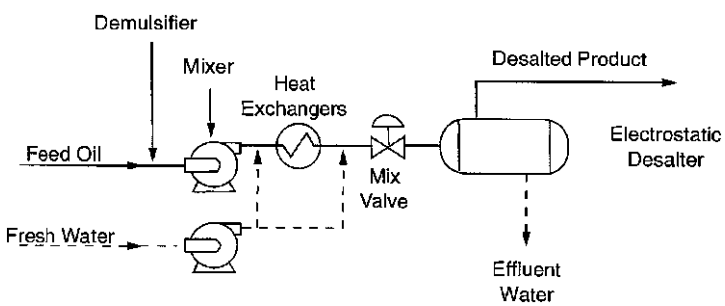

Figure 19-13 Desalting process.

Optimum mixing of fresh water is desired for satisfactory desalting. Poor mixing can lead to carryover of salt in the crude, which causes:

- Fouling of heat exchangers
- Coking of furnace tubes
- Excessive corrosion of downstream equipment
- Poisoning of catalysts in downstream processes

Overmixing can result in the formation of a stable emulsion and poor separation. Water carried over and oil carried under can cause:

- Water flashing in the pipestill and hydrocarbon release into the atmosphere
- Poor product quality
- Loss of hydrocarbon value
- Effluent water contamination and disposal problems

Conventional in-line mixers used for mixing fresh water in oil include mixing valve, variable speed multistage mixing tank (Figure 19-7), and static mixers (Figure 19-5*b–d*). The first two mixer types are used more commonly because the mixing energy can be adjusted depending on the flow rate. This mixing energy must be optimized for adequate removal of salt without water carryover. The desalter operating data shown in Figure 19-14 indicate that as the mixing valve pressure drop is increased, salt concentration in the oil decreases rapidly and water carryover increases slowly. However, if pressure drop is increased to above a critical value, water carryover increases rapidly, which is then followed by increase in salt carryover. This performance plot depends on crude type, temperature, and demulsifier type. Continuous monitoring of BS&W in the

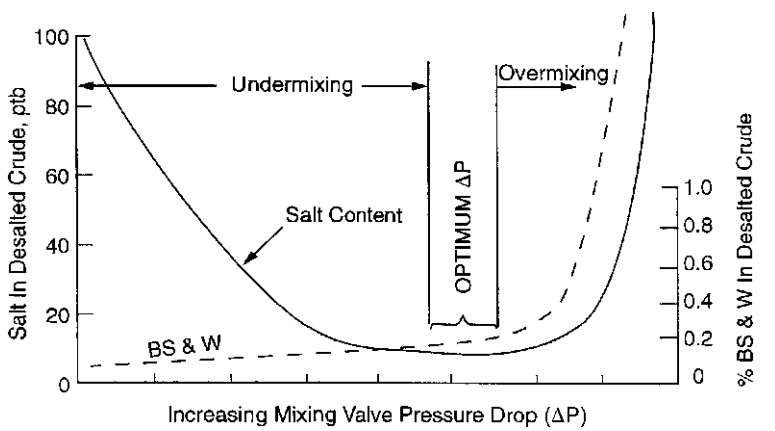

Figure 19-14 Optimizing mixing valve pressure drop in desalting.

crude product, coupled with mix valve adjustment, is necessary to ensure high performance level.

19-7 ALKYLATION

Alkylation is a process for producing high-octane hydrocarbons with acid-catalyzed exothermic reactions of C_4 and C_5 olefins. The process can be based on HF or H_2SO_4. With the H_2SO_4 process, two configurations are used depending on the heat removal method, autorefrigeration, and indirect refrigeration (Figure 19-15). This process requires adequate contacting of hydrocarbons with concentrated sulfuric acid for a primary fast reaction and several parallel and consecutive secondary reactions. In the autorefrigerated system, heat is removed by boiling a hydrocarbon.

Good mixing in the reactor is important for producing a hydrocarbon-in-acid dispersion at minimum energy consumption and high mass transfer rate but short settling time. Excessive energy consumption can increase the load on refrigeration, and a stable emulsion can form and cause acid carryover and corrosion in the downstream equipment. The mixing system should be suitable for producing narrow distribution of drops. Such dispersion quality is desired for fast settling rates. Two types of impellers are used in commercial alkylation reactors, turbines, and hydrofoils. Both types result in nearly the same reaction yield when designed at 5.0 hp/kgal. However, the drop size distribution with hydrofoils is somewhat narrower than with turbines and can be better for minimizing acid carryover. Adequately designed static mixers are also used downstream of the reactor for neutralization of entrained acid by contacting with caustic.

19-8 OTHER APPLICATIONS

In addition to the applications discussed above, there are several other areas where mixing is important. They include suspension of catalyst fines in storage tanks for

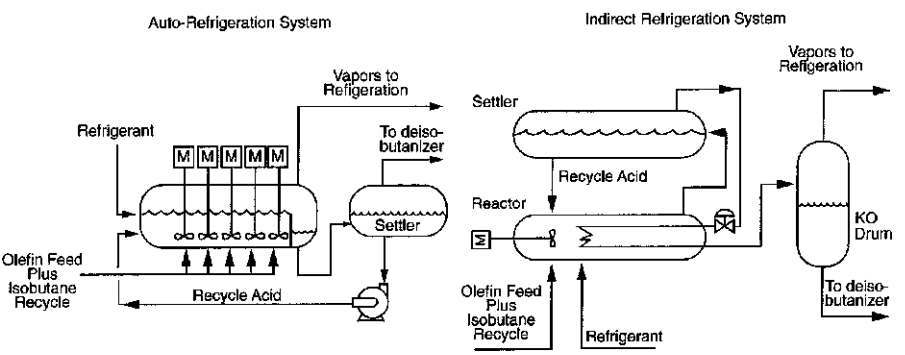

Figure 19-15 Sulfuric acid catalyzed alkylation processes.

catalytic fractionator bottoms, product blending tanks, caustic treat/water wash of hydrocarbons for corrosion control, caustic contacting of gasoline for removal of elemental sulfur, and more. Although refineries have mixing systems in use, they are often designed on the basis of limited data and experience and can be inadequate. Therefore, design guidelines are needed for mixing systems to achieve good process performance and reliability. Other chapters in this book provide some of these design guidelines.

NOMENCLATURE

ΔP	pressure drop
d	drop size of dispersion
D	pipe diameter
E_m	total energy per unit mass
f	friction factor
Q	volumetric flow rate
R	cleaning radius
S	specific gravity
v	velocity
V	mixer volume
We	Weber number $\frac{ev^2D}{\sigma}$

Greek Symbols

ρ	liquid density
θ	interfacial tension

REFERENCES

Fasano, J. B., and D. C. Ryan (1988). Presentation at the AIChE 1988 Annual Meeting, Washington, DC.

JISKOOT, Inc., Houston, TX, technical literature.

Neyrtec, France, technical literature.

Sarp UK Ltd., private communications on P-43 jet mixers.

CHAPTER 20

Mixing in the Pulp and Paper Industry

CHAD P. J. BENNINGTON
University of British Columbia

20-1 INTRODUCTION

Since its invention in A.D. 105, paper use has steadily grown to become the world's preferred media for information dissemination and storage. Today, pulp and paper products cover a wide spectrum, from hygiene items, through a myriad of paper grades, to packaging materials. Pulp and paper production is a major and diversified world industry. In 2000, 188 million metric tons of pulp and 323 million metric tons of paper and paperboard were produced, with major production in Canada, the United States, and the Nordic countries (Pulp and Paper International, 2001). Paper is a renewable resource, and with proper stewardship, world demand can be met indefinitely. Part of this involves reuse of paper products. Recycling programs in many countries recover over 50% of their paper each year for inclusion in new products (FAO, 1999).

The demand for pulp and paper products continues to grow. Growth has typically been linked to gross national product levels, with developing countries using more paper per capita as standards of living rise. However, the emergence of new information technologies is changing the demand for paper. The success and acceptance of these technologies will determine the extent to which individual paper products will be affected. In the short term, demand for high-quality print-on-demand paper grades has increased. On longer time frames, demand for newsprint is forecast to decrease and that for packaging grades to increase.

The diverse range of paper products available necessitates a variety of pulp production processes. These range from mechanical to chemical processes, each producing pulps with unique attributes. These pulps are then blended to craft paper products having the desired properties for their end use.

Handbook of Industrial Mixing: Science and Practice, Edited by Edward L. Paul, Victor A. Atiemo-Obeng, and Suzanne M. Kresta
ISBN 0-471-26919-0

The most common chemical pulping process is the kraft process. Here, wood chips are treated to remove the lignin that binds the cellulose fiber to the wood matrix. Once released as individual fibers, residual lignin (which is also a chromophore) is progressively removed through a series of increasingly selective delignification and bleaching/brightening steps. Bleached kraft pulp can then be mixed with other pulps (and with minerals and additives) to produce any number of paper products, including the paper used to produce this book. The kraft process is the dominant chemical pulping process, due to the strength of the pulp it produces and the fact that an effective chemical recovery scheme exists. Process details may be found in a number of reference books, including Grace and Malcolm (1989), Smook (1992), Biermann (1996), and Gullichsen and Fogelholm (1999).

Mixing is an essential unit operation in all facets of pulp and paper manufacture. The range of mixing applications is extensive. These include examples from liquid–liquid to gas–solid–liquid mixing, from the blending of complex fluids to the mixing of reactive chemicals. For pulp fiber suspensions, mixing processes include blending pulp streams for papermaking, addition of wet-end and other chemical additives prior to sheet forming, consistency control ahead of most papermaking and pulp processing stages, and chemical contacting in pulp bleaching operations. Figure 20-1 is a typical process flow diagram for kraft pulp production. The NAMF (North American Mixing Forum) logo indicates those unit operations where mixing is important.

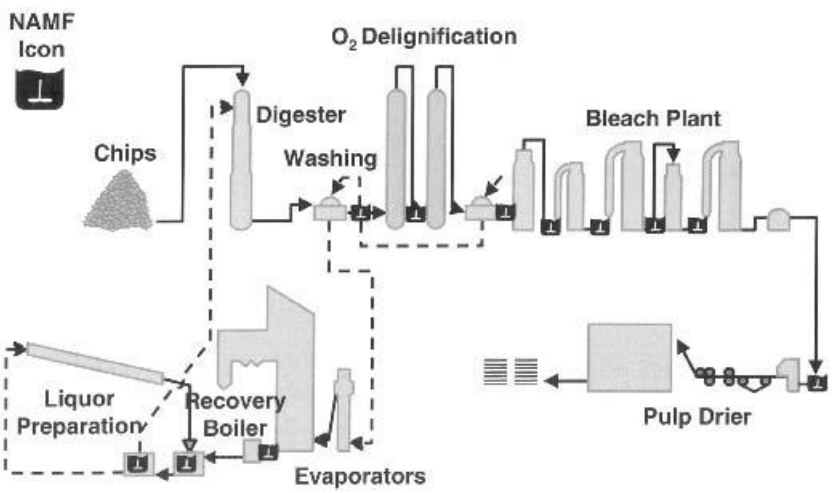

Figure 20-1 Simplified overview of a typical kraft process showing chemical pulping, oxygen delignification, pulp bleaching, and chemical recovery systems. Important mixing operations are indicated by the NAMF mixing icon.

20-2 SELECTED MIXING APPLICATIONS IN PULP AND PAPER PROCESSES: NONFIBROUS SYSTEMS

Examples of mixing applications in pulp and paper processes are given below. They were selected to illustrate both the unique and diverse applications of mixing in pulp and paper technologies, and the critical role that mixing plays in pulp and paper manufacture. The examples have been classified under the traditional mixing disciplines and are not meant to be exhaustive.

20-2.1 Liquid–Liquid Mixing

Liquid–liquid mixing is common for chemical preparation in various pulp and paper processes. The dilution and makeup of bleaching solutions is done routinely using stirred vessels or static mixers. Applications of this type are discussed in other chapters.

One unique liquid–"liquid" mixing application is smelt dissolving. Molten smelt (molten salt at about 900°C) is added to a weak wash to form a green liquor (a green aqueous solution of Na_2S and Na_2CO_3) in the recovery cycle. The smelt stream is "shattered" using steam jets to avoid large clumps of smelt entering the water and creating an explosion. The smelt solidifies on contact with the water and must be dissolved to produce the green liquor. Vigorous mixing is required to ensure solids suspension and dissolution. Stagnation zones must be avoided to prevent forming zones of high concentration that would lead to scaling problems (Frederick et al., 1990). The industry standard is to achieve this in baffled stirred tank reactors having a large fluid circulation (Holman et al., 1989; Ljungqvist and Theliander, 1995). Air entrainment, which would reoxidize the sodium sulfide generated by reduction in the furnace, must be avoided. Recent work has used computational fluid dynamics (CFD) and laboratory scale modeling to examine impeller configurations and mixing conditions to minimize the mixing time (Ljungqvist and Theliander, 1995).

20-2.2 Gas–Liquid Mixing

20-2.2.1 White and Black Liquor Oxidation. White liquor is an alkaline solution of sodium sulfide (Na_2S) and sodium hydroxide (NaOH) used to react with and remove lignin from wood chips during a kraft cook. Black liquor is the liquor separated from the pulp following the cook and contains the unreacted (residual) cooking chemicals and dissolved wood components. Both the white and black liquors contain Na_2S, which requires oxidation at certain points in the kraft process.

Black liquor is concentrated and incinerated to recover and regenerate the pulping chemicals and to utilize the heating value of the dissolved wood components. During liquor processing, older-style recovery furnaces use the sensible

heat of the flue gas to evaporate water from the liquor. This is achieved in direct-contact evaporators. However, carbon dioxide in the flue gas reacts with sodium sulfide in the liquor (hydrolyzed to HS^- under the alkaline processing conditions) to release hydrogen sulfide into the gas stream:

$$HS^- + CO_2 + H_2O \rightarrow HCO_3^- + H_2S \tag{20-1}$$

To prevent release of this pollutant, the liquor is oxidized to convert the Na_2S to thiosulfate ($Na_2S_2O_3$). The oxidation reactions can be written as

$$2HS^- + 2O_2 \rightarrow S_2O_3^{2-} + H_2O \tag{20-2}$$

$$S_2O_3^{2-} + 2O_2 \rightarrow SO_4^{2-} + H_2O \tag{20-3}$$

In black liquor oxidation, it is important to oxidize the sulfide but not to overoxidize the liquor and reduce its heating value. Consequently, target levels of sulfide in the strong black liquor going to the furnace are typically <0.1 g/L.

Industrial implementation of black liquor oxidation recognized the importance of effective gas–liquid mass transfer in the reaction. Sparged tank reactors are often used, with compartmentalized reaction zones to optimize reactor size given the reaction kinetics (Morgan and Murray, 1971; Shaw and Christie, 1984). Pipeline reactors can also be used to oxidize black liquor but gas–liquor mass transfer is critical and it may be necessary to increase the gas–liquid mass transfer by using static mixers in some applications.

White liquor is oxidized, so it may be used as a source of caustic in oxygen delignification and alkali extraction stages in the bleach plant. The degree of oxidation determines where the liquor can be used. Partially oxidized liquor can be used for oxygen delignification where reaction conditions do not oxidize the thiosulfate ($S_2O_3^{2-}$) remaining in the liquor. Fully oxidized liquor has all thiosulfate converted to sulfate. This liquor can be used in alkaline extraction stages reinforced using hydrogen peroxide. Under the reaction conditions of a peroxide-reinforced extraction stage, the peroxide would oxidize any thiosulfate remaining in the liquor and be wasted.

White liquor oxidation occurs under more severe reaction conditions than black liquor oxidation. Again, gas–liquid mass transfer is essential, and several reactor designs have been used for this purpose, including sparged stirred vessels, pipeline reactors (Thring et al., 1995), and buss loop reactors.

20-2.2.2 Generation of Alkaline Peroxymonosulfate. Alkaline peroxymonosulfate (Na_2SO_5 or PMS) is a bleaching chemical that has been used successfully to augment delignification in the laboratory. In conjunction with oxygen, the addition of 1.0% PMS to an oxygen delignification system (on an active oxygen basis) increased delignification from 49% to 73% without reducing pulp strength (Bouchard et al., 2000). However, the commercial implementation of PMS requires an efficient and cost-effective strategy for its generation. One promising method of achieving this is the catalytic oxidation of sodium sulfite

with oxygen. Laboratory generation of PMS is readily achieved by this route, but typically at low yields (<20%) and low concentrations (<3.8 g/L).

The exact reaction mechanism for peroxymonosulfate generation using the copper-catalyzed sulfite oxidation is open to interpretation. The possible reaction mechanisms given in the literature can be simplified to the following reactions:

$$SO_3^{2-} + O_2 \xrightarrow{Cu^{2+}} SO_5^{2-} \tag{20-4}$$

$$SO_5^{2-} + SO_3^{2-} \rightarrow 2SO_4^{2-} \tag{20-5}$$

$$SO_5^{2-} \rightarrow 0.5O_2 + SO_4^{2-} \tag{20-6}$$

where PMS is produced by the catalytic oxidation of sulfite, but once produced can be reduced to sulfate by sulfite. In addition, peroxymonosulfate can decompose. If we ignore the decomposition reaction, which is slow, eqs. (20-4) and (20-5) represent a classic consecutive-competitive reaction scheme.

Studies conducted where PMS was generated under systematically varied mixing conditions (stirred tank reactor, semibatch reaction mode with sulfite maintained as the limiting reagent) showed the classic dependence of yield on sulfite feed time, chemical concentration, and mixing intensity. By adjusting mixing conditions, PMS yield was increased to 32.5% at 9.8 g/L and to 54% at 1.6 g/L (Shaharuzzaman and Bennington, 2001). The experimental results followed the E-model predictions of Baldyga and Bourne (1989) over the energy dissipation range studied, as shown in Figure 20-2. However, as power input

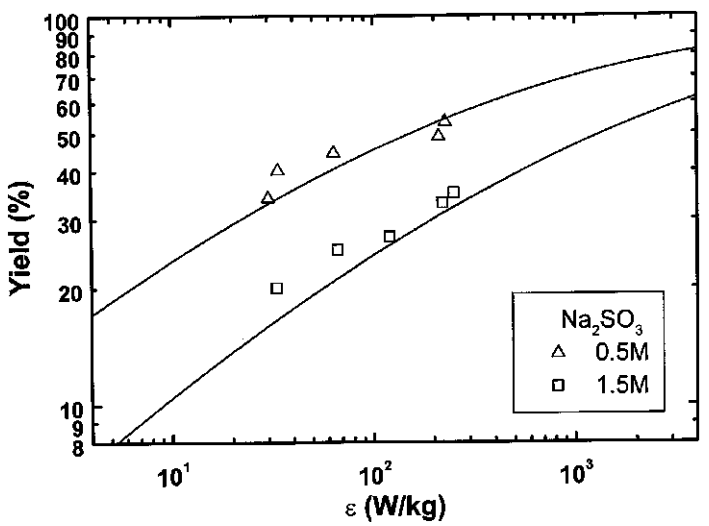

Figure 20-2 Peroxymonosulfate yield versus average energy dissipation during reaction. The lines give micromixing predictions [with the E-model of Baldyga and Bourne (1989) using fitted rate constants].

increased, local gas–liquid mass transfer became insufficient to maintain the local oxygen concentration in excess and restricted the yield gain. Despite the improved generation efficiency, yields are still too low for economic implementation of peroxymonosulfate industrially. Further research may improve the economic feasibility of PMS use, while the results obtained demonstrate the role mixing can play improving generation of bleaching chemicals.

20-2.3 Solid–Liquid Mixing

Examples of solid–liquid mixing are found in kraft chemical recovery and in papermaking. In the recovery furnace, particulate material is removed from the boiler flue gases as dry solids and mixed with concentrated black liquor prior to reintroduction to the furnace. In coated papermaking production, coating preparation is critical for paper performance and uniformity. In chemical recovery, the recausticizing operation is an essential process for white liquor preparation and relies on effective solid–liquid mixing.

20-2.3.1 Preparation of Coating Colors. Coating colors are concentrated slurries (of pigments, binders, and additives) applied to the surface of paper to enhance paper properties and print quality. The slurry concentration is as high as possible (often as high as 70% by mass) to limit the effect of moisture uptake (rewetting) on paper structure and to minimize the extent of subsequent paper drying required. Only as much water as required to achieve the desired flow properties of the coating color should be used.

The preparation of the coating formulation is extremely important (Robinson et al., 1997; Makinen, 1999; Thibault, 1999), as coating properties (especially their rheology) depend on the mixing applied. A wide range of specialized mixers that can operate over the wide range of process conditions encountered during coating preparation have been developed.

Several steps are used in coating preparation. The first involves preparing a pigment slurry from dry powder. This requires wetting the pigment. Two methods are used for this: forming a vortex in the mixer to draw the pigment into the slurry or using a rotor on the liquid surface to incorporate the dry pigment with the slurry. The power required for mixing increases significantly with increasing slurry solids content during this make-down period. Often, the slurry approaches the limit of fluid behavior. The slurry must then be homogenized, with any lumps and aggregates formed during powder addition removed by the erosion or fracture of the particles. This is achieved by applying shear during mixing, although dispersants can be added to aid this process. The power level falls as the suspension becomes homogenized. Several mixer types are used in this application, including the Cowles turbine, rotor–stator mixers (e.g., the Kady Mill), kneaders, and coaxial agitators. The coaxial agitators use two different impellers, each with its own motor, for mixing the dispersion. The central agitator is a high-speed turbine designed to mix and disperse the pigment. The outer agitator turns at low speed in proximity to the vessel wall to ensure that the

entire suspension is well mixed. The two agitators can be rotated cocurrently (Ekato) or countercurrently (Cellier) (Thibault, 1999).

The effect of mixing (time and intensity) on the rheology of the pigment slurry is summarized by Robinson et al. (1997). Breakdown of the dispersion agglomerates requires imposition of shear on the slurry. Consequently, the impeller tip speed is critical for disperser operation and mixer design. As the maximum shear rate [ranging from 100 to 10^4 s^{-1} in dispersion operations (Makinen, 1999)] determines the ultimate size of the particles, extending the dispersion time cannot compensate for an inadequate shear level.

The second step in coating preparation is the coating formulation. The dispersed pigment is mixed with appropriate binders and cobinders (adhesives, such as starches and latexes) and other additives (optical whiteners and viscosity modifiers) to achieve the properties required for the coating. The quantity of materials and their order of addition greatly influences the ease of mixing and the properties and quality of the final color preparation (Makinen, 1999). The order in which the coating components are added determines their interaction with each other, and consequently, the size of the pigment particles and the rheology of the slurry. Certain components, if added in a particular order, rapidly form viscous mixtures that suddenly and dramatically increase the load on the mixer, placing unacceptable loads on it. Continued mixing may reduce the overall mixture viscosity as slurry aggregates are comminuted by shear during mixing. However, the final quality (rheology) of the color may not be an optimum. Once prepared, coating colors are kept in motion, by either mixing or recirculation, until applied to paper in a coating nip, where the shear rate can approach 10^6 s^{-1}.

20-2.3.2 Causticization. White liquor is prepared by mixing green liquor (largely sodium carbonate, Na_2CO_3) with calcium oxide (CaO). The calcium oxide slakes with water to form calcium hydroxide, $Ca(OH)_2$, which then reacts to produce sodium hydroxide:

$$CaO(s) + H_2O \rightarrow Ca(OH)_2(s) \tag{20-7}$$

$$Ca(OH)_2(s) + Na_2CO_3(aq) \Leftrightarrow 2NaOH(aq) + CaCO_3(s) \tag{20-8}$$

The reaction occurs in the solid pellets of CaO, governed by a shrinking core reaction mechanism. Consequently, particle size affects reaction progress, its yield (extent of unreacted material, referred to as *deadload*), and the ease of the subsequent separation of $CaCO_3$ from the system. The reaction is initiated in a slaker where calcium oxide is mixed into hot green liquor. The slaking reaction [eq. (20-7)] is strongly exothermic and completed in 10 to 15 min. The suspension is then passed through a series of causticizers (stirred tank reactors) to permit the equilibrium of eq. (20-8) to be established. A total residence time of 90 to 150 min is needed for this, and plug flow is desirable to limit short-circuiting of the solid phase. Short-circuiting would permit unreacted $Ca(OH)_2$ to reach the clarification stage, increasing system deadload and leading potentially to mud-settling problems. Typically, three or four stirred tanks in series are used,

and the tanks can be compartmentalized to more closely approach plug flow. The causticizers use various impellers, with the goal of achieving well-mixed compartments and full suspension of the solids. The impeller tip speed is the most common criterion used by equipment manufacturers for both slaker and causticizer scale-up and is not varied during operation. Although increased mixing intensity can increase the rate of causticization slightly, it can dramatically affect the settling rate of the calcium carbonate particles, largely by reducing particle size (Dorris, 2000). Laboratory studies made by Dorris used a series of impellers to confirm that particle size decreased and filtration resistance increased with increased impeller tip speed. The absolute values depended on the specific impeller used. When the data were compared in terms of the average power dissipation in the vessel, filtration resistance depended only on the power input and the impeller/tank diameter ratio.

20-2.4 Gas–Solid–Liquid Mixing

20-2.4.1 Polysulfide Generation. Polysulfides, linear oligomers of sulfur (S_nS^{-2}, where n = 1 to 4), protect hemicelluloses during kraft cooking. This results in a significant increase in pulp yield if added during the cooking process. Polysulfides can be produced by the oxidation of sodium sulfide in the white liquor (hydrolyzed to HS^-) by oxygen in the presence of a catalyst (e.g., activated carbon or MnO_2). The reactions are complex and the mechanisms unknown. However, they can be represented by (Dorris and Uloth, 1994)

$$(2n+2)HS^- + nO_2 \longleftrightarrow 2S_nS^{2-} + 2(n-1)OH^- + 2H_2O \qquad (20\text{-}9)$$

$$nS_nS^{2-} + H_2O \longleftrightarrow (n-1)S_nS^{2-} + HS^- + OH^- \qquad (20\text{-}10)$$

with equilibrium established between polysulfide species of various chain lengths to give an average length, n, of 2.4 for typical reaction conditions (Dobson, 2001).

The polysulfide generated can be oxidized to thiosulfate:

$$2S_nS^{2-} + (n+2)O_2 + 2(n-1)OH^- \rightarrow (n+1)S_2O_3^{2-} + (n-1)H_2O \qquad (20\text{-}11)$$

reducing the polysulfide yield.

The Paprilox® process catalytically oxidizes sulfide (present in the white liquor) to polysulfide during the causticization reaction (Uloth et al., 1996). Here, air or oxygen is sparged into one (usually, the last) causticizer, giving about 60 min for polysulfide generation. The impeller is used to create gas–liquid surface area, mix the gas throughout the vessel, and suspend the solids (the lime mud and added MnO_2 catalyze the oxidation). Mill implementation of the polysulfide process indicated sensitivity to mixing conditions (Uloth et al., 1996). Recent laboratory work (Dobson and Bennington, 2002) confirmed that mixing could alter the reaction rate, yield, and selectivity of polysulfide generation. For example, Figure 20-3 shows the effect of impeller speed on polysulfide selectivity

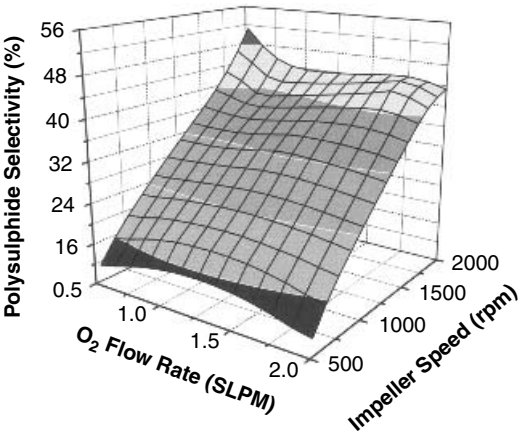

Figure 20-3 Polysulfide selectivity (maximum selectivity achieved during 100 min of reaction) versus impeller speed and oxygen flow rate. Generation in a laboratory sparged stirred-tank reactor at $T = 90^{\circ}C$ using 2.0 g/L of Fisher MnO_2 catalyst. Selectivity is the fraction of polysulfide (as g S°/L) formed divided by the hydrosulfide ion consumed during oxidation (as g S/L). (From Dobson and Bennington, 2002.)

in a laboratory sparged-tank mixer. For fixed reaction conditions (reactant concentrations, temperature, etc.), increasing the impeller speed increased both the rate of polysulfide formation and the maximum polysulfide concentration reached during reaction. For the catalyst studied, the peak yield of polysulfide could be increased from 1.2 to 9.6 g/L (expressed as S°) as impeller speed increased from $N = 500$ to 2000 rpm. However, caution must be exercised when adjusting mixing to optimize oxidation in the mill. Any increased turbulence could increase the settling time of the lime mud and impair the clarification step that follows recausticizaton.

One final example of gas–liquid–solid mixing is the flotation process used in paper deinking operations. Ink is detached from fiber surfaces in the previous repulping operation, with ink redeposition minimized by creating an appropriate chemical environment. Air is used to collect the ink particles in the low consistency pulp suspension ($C_m < 0.01$) and float them to the surface where they are removed with the froth. Operating conditions are created to minimize entrapment of fiber in the rising bubble stream. The ink collection efficiency depends on the combined probability of a number of sequential events: collision between an ink particle and gas bubble, ink adhesion to the bubble, and maintenance of the ink–air bond. Mixing is critical for all these processes. The turbulence created in mixing determines the gas bubble size and creates interactions between the ink particles and bubbles that lead to collisions. The probability of adhesion depends on the magnitude of the inertial forces created in the flow. These forces must be strong enough to allow ink particles to penetrate the flow streamlines and approach the bubble surface, but it must not be so vigorous as to detach the ink particles once attached (Somasundaran and Zhang, 1998).

Industrial flotation cells use a variety of strategies to create bubble surface area and contact it with the suspension. These include mixing the gas (typically 10 to 20 vol %) with the suspension in some manner. Injector nozzles, turbines, or impellers can be used for this purpose. No well-defined criteria are published for designing gas/suspension mixing in flotation systems. However, all the mixing/contacting strategies attempt to create small gas bubbles and ensure efficient bubble/suspension contact in a well-mixed zone. This is followed by a quiescent zone in which the gas (and the attached ink) can readily separate from the suspension (McKinney, 1998).

20-3 PULP FIBER SUSPENSIONS

20-3.1 Pulp Suspension Mixing

Pulp suspensions must be mixed in many applications. For example, in papermaking many additives are mixed with pulp before sheet forming. These include a variety of wet-end chemicals, such as retention aids, antislimming agents, filler materials, and dyes. To be effective, these must be mixed uniformly throughout the suspension. Since wet-end processing is normally conducted at low suspension concentrations, mixing is readily accomplished with agitated chests. However, the unique rheology of the fiber suspensions, even at these low mass concentrations, creates challenges during mixing. As the suspension mass concentration increases, mixing becomes even more difficult. Consequently, characterizing and understanding suspension behavior is critical when designing pulp mixing systems.

20-3.2 Characterization of Pulp Suspensions

Pulp suspensions are composed of an array of wood components, including parenchyma cells, fibers, tracheids, and vessel elements, although the main components of interest are the fibers and tracheids. Individual fibers are small. A typical softwood tracheid (in wood) has a length of 3 to 7 mm, a width of 24 to 59 μm, and a cell wall thickness of 2 to 7 μm (Rydholm, 1965). After processing, the fiber length is reduced and the fiber lumen partially or fully collapsed. Following mechanical processing (using stoneground wood or thermomechanical pulp processes) the typical length-weighted fiber length, l_w, of a mill-produced hemlock–balsam pulp is 0.6 to 1.2 mm. The same fiber following chemical processing (e.g., the kraft process) would have a l_w value of 1.9 to 2.4 mm (Bennington, 1988).

In suspension, fibers form coherent networks, which are interconnected systems with fibers in continuous contact with other fibers (see Figure 20-4). Forces exist at the fiber contact points, creating fiber aggregates (flocs) and giving the network mechanical strength. Before motion can be initiated within a suspension, whether to mix, transport, or disperse flocs, external forces sufficient to overcome the network forces must be applied.

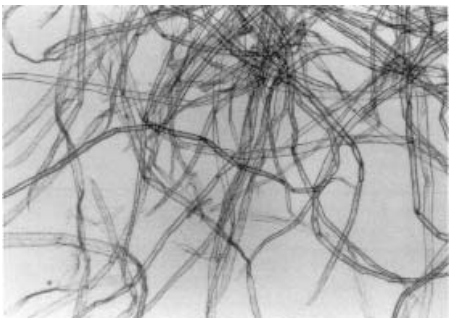

(*a*)

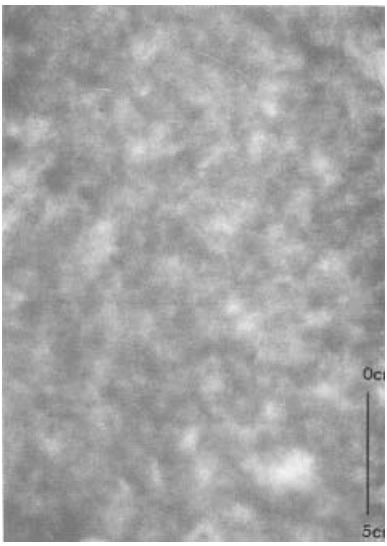

(*b*)

(*c*)

Figure 20-4 Photographs of fibers and suspensions: (*a*) photomicrograph of softwood trachieds ($l_w = 2.37$ mm); (*b*) light transmission through a $C_m = 0.005$ kraft pulp suspension showing mass nonuniformities (flocs). The line in the image is 5 cm in length; (*c*) hands hold a medium consistency ($C_m = 0.10$) kraft pulp suspension. See insert for a color representation of this figure.

Pulp suspensions are often characterized by two factors. The length-weighted fiber length is often used as a single parameter to characterize the average length of fibers within the suspension. The fiber length distribution is very broad (often extending two decades in length), and the length-weighted average provides greater weighting to the longer fibers, which disproportionately influence suspension behavior.

The mass concentration of the suspension, C_m, specifies the mass of fibers in the suspending medium, which is usually water. Thus,

$$C_m = \frac{m_f}{m_f + m_w} \tag{20-12}$$

where m_f and m_w are the mass of fiber and water, respectively. This parameter is commonly used industrially (where it is referred to as the *consistency* of the suspension and often expressed as a percentage) to calculate production and chemical

applications. Throughout this chapter, unless otherwise specified, the mass concentration is expressed as a fraction. Suspension rheology changes dramatically with mass concentration, varies widely among pulp and paper unit operations, and is typically categorized as being low ($C_m < 0.04$), medium ($0.08 \leq C_m \leq 0.16$), or high ($C_m > 0.20$) in pulping and bleaching operations.

The volume concentration of a pulp suspension, C_v, gives a better indication of suspension behavior, although it is not always easily calculated. Pulp fibers are hollow, and the lumen volume changes with the degree of mechanical action and the chemical treatment experienced during processing. The cell wall material also absorbs considerable water, causing fiber swelling and increasing fiber volume. Thus, calculation of the suspension volume concentration requires specification of at least two additional parameters: the quantity of water absorbed by the cell wall and the volume of the fiber lumen.

The degree of fiber collapse has only recently been measured (Jang and Seth, 1998). Fiber collapse, and hence lumen volume, has not been widely characterized as a function of fiber type or processing history and is presently a time-consuming measurement. However, the adsorption of water by the cell wall has been studied extensively. It can be measured by two tests, a solute exclusion test that yields the fiber saturation point and a water extraction test using a centrifugal field that yields the water retention value. Both tests can be used to estimate the amount of water responsible for fiber swelling, X_w, and agree over a range of test conditions (Scallan and Carles, 1972). Values for X_w depend on pulp type and processing history, and for a typical kraft pulp can range from 0.8 to 2.0 kg water/kg fiber (Scallan and Carles, 1972). For a completely collapsed fiber (a reasonable approximation for a fully bleached kraft pulp) at low mass concentrations ($C_m \leq 0.04$ and where the gas trapped in the suspension is negligible), C_v can be calculated using (Bennington et al., 1990)

$$C_v = \frac{1 + X_w(\rho_f/\rho_w)}{1 + [(1 - C_m)/C_m](\rho_f/\rho_w)} \tag{20-13}$$

where ρ_f is the density of the cell wall material ($\rho_{cellulose} = 1500$ kg/m^3) and ρ_w is the density of water. If gas is present in the suspension, which can occur at any suspension mass concentration but is common for $C_m > 0.08$, some measure of the gas volume must also be known to compute C_v. For example, if the bulk density of the suspension, ρ_b, is known,

$$C_v = C_m \left(\frac{1}{\rho_f} + \frac{X_w}{\rho_w} \right) \rho_b \tag{20-14}$$

Fiber suspensions are never uniform. They aggregate to form mass concentrations within the suspension, called *flocs* (Kerekes et al., 1985). These form even at low mass concentrations, as shown in Figure 20-4*b*. In various unit operations, fiber flocs must be disrupted and dispersed. The uniformity of a paper surface, called its *formation*, depends largely on floc dispersion during sheet formation

in papermaking. Bleaching efficiency, particularly at higher mass concentrations, depends on floc dispersion during mixing with reactive chemicals. The latter can be difficult to achieve at typical bleaching processing conditions. Medium consistency pulp suspensions ($0.08 \leq C_m \leq 0.16$) are a case in point. As shown in Figure 20-4*c*, a $C_m = 0.10$ suspension, despite being 90% water by mass, displays solidlike behavior.

20-3.3 Suspension Yield Stress

Before motion can be initiated in a suspension, the yield stress must be overcome. Due to floc formation, the suspension first yields in low-strength regions between flocs. Thus, flow occurs before floc disruption. Suspension yield stress increases dramatically with concentration. At low mass concentrations ($C_m < 0.04$), where the gas content is negligible, the yield stress has been given traditionally by expressions of the form

$$\tau_y = aC_m^b \tag{20-15}$$

where τ_y is the suspension yield stress, C_m the mass concentration, and a and b are parameters that depend on pulp type and processing history. Kerekes et al. (1985) found that the exponent, b, varied from 1.69 to 3.02. A more general correlation encompassing a wider range of pulps can be made using the volume concentration, C_v:

$$\tau_y = aC_v^b \tag{20-16}$$

which also accounts for the presence of gas within the suspension. Bennington et al. (1995) correlated an extensive set of experimental data to arrive at

$$\tau_y = 7.7 \times 10^5 C_m^{3.2}(1 - \phi_g)^{3.4} A^{0.6} \tag{20-17}$$

which expresses yield stress as a function of the mass concentration (expressed as a fraction), the void fraction of gas in suspension, ϕ_g, and the aspect ratio of the fiber, A. The agreement between this equation (for $A = 70$) and extensive network strength data from the literature is given in Figure 20-5 (Bennington et al., 1995). The equation accounts for the observed dependency of suspension mass concentration, gas void fraction, and fiber aspect ratio displayed by a range of fiber networks, although a correlation developed for an individual pulp fiber would be more accurate.

Suspension yield stress must be considered in mixer design. Ideally, we want motion to exist throughout a mixing vessel, with no stagnation or dead zones present. As illustrated in Figure 20-6, this can be difficult to achieve. Here a $C_m = 0.02$ fully bleached kraft fiber suspension was agitated in a stirred vessel using a Rushton turbine. Dye was added to indicate regions of suspension motion. In Figure 20-6*a* the impeller was rotating at $N = 4$ rps. No motion was detected at the vessel wall. As impeller speed was increased to $N = 7$ rps, motion became apparent throughout most of the vessel volume, but stagnant regions existed in the

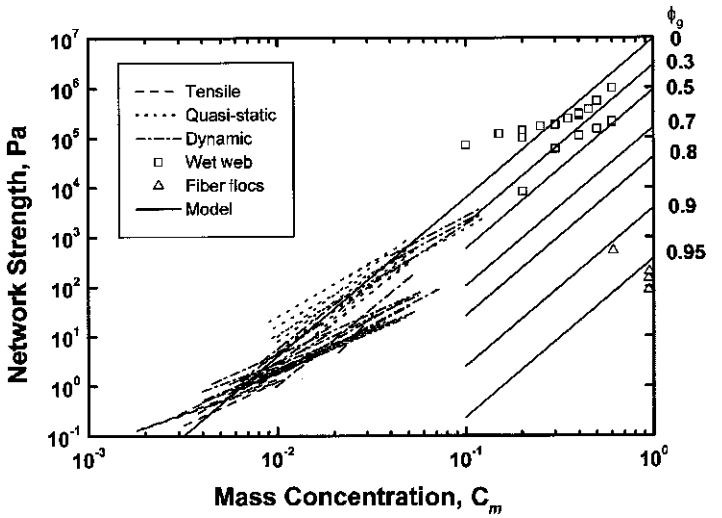

Figure 20-5 Fiber network strength versus suspension mass concentration. Compilation of literature data. The predictions of eq. (20-17) for a fiber having an aspect ratio of A = 70 are given.

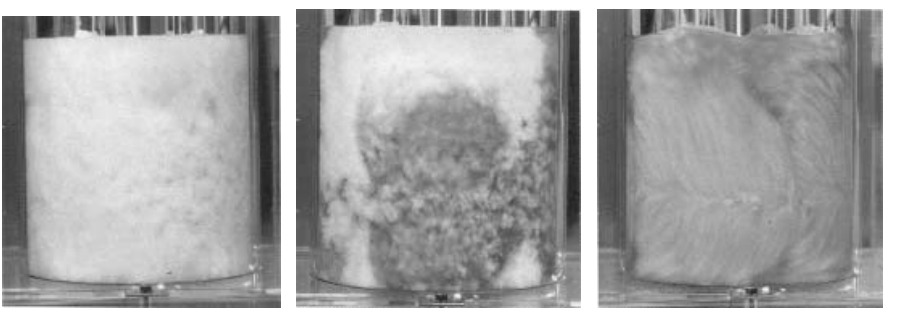

(*a*) (*b*) (*c*)

Figure 20-6 Effect of yield stress on suspension motion in a stirred tank. $C_m = 0.02$ FBK suspension. The vessel is 30 cm in diameter with the suspension height set at 30 cm. A D = 10 cm diameter Rushton turbine was located 10 cm from the vessel floor. Impeller speeds are N = (*a*) 4, (*b*) 7, and (*c*) 14 rps. The red dye shows regions of suspension motion. In image (*a*) the cavern has not reached the vessel wall. See insert for a color representation of this figure.

low-shear regions at the wall. Increasing impeller speed to N = 14 rps produced motion throughout the vessel, but a wide range in local suspension velocity was apparent. The dramatic increase in network strength with mass concentration (Figure 20-5) means that the yield stress becomes more important for mixing as suspension concentration increases.

Yield stress fluids create caverns around impellers. The cavern boundary is delineated by the surface where the imposed shear force does not exceed the fluid yield stress. Pulp suspensions exhibit this behavior. The approach developed by Soloman et al. (1981) was used to characterize pulp suspension behavior in a laboratory mixer. A force balance at the cavern boundary (assumed cylindrical) gives its radial extent, r_a, as

$$r_a = \sqrt{\frac{T}{2\pi\tau_y L}} \tag{20-18}$$

where T is the measured torque, L the length of the cylindrical rotor, and τ_y the suspension yield stress. The cavern size measured for fully bleached kraft (FBK) pulp suspensions having mass concentrations from $C_m = 0.042$ to 0.095 is compared with predictions of eq. (20-18) in Figure 20-7 (Bennington, 1988). The results show that the equation underpredicts the cavern size. The accuracy with which the cavern radius could be measured and the accuracy of the yield stress determination are significant, as indicated by the error bars on the graph, and explain some of the discrepancy. The extent of suspension motion is important for operation of agitated chests but is difficult to predict.

20-3.4 Turbulent Behavior of Pulp Suspensions

Continued disruption of the fiber network is necessary to create and maintain suspension motion. This requires continuous application of force sufficient

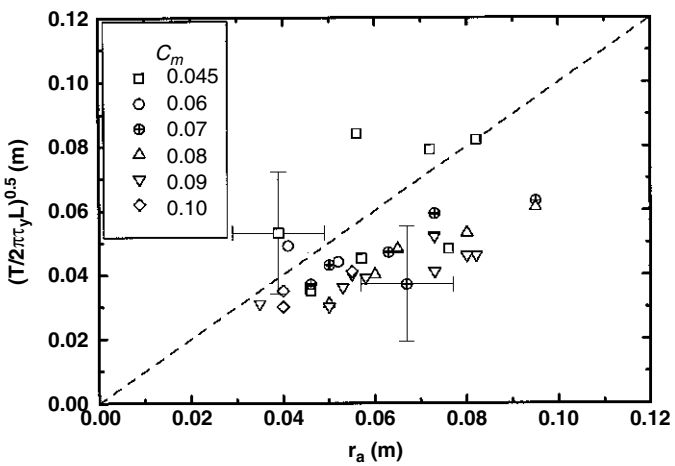

Figure 20-7 Measured cavern radius versus that predicted using eq. (20-18) for tests made using a fully bleached kraft pulp. The test apparatus has a horizontal Couette geometry. The housing has a depth of 10 cm and a diameter of 22 cm. Six 1 cm baffles are spaced at 60° intervals around the periphery to limit slip at the vessel wall. The rotor is six-bladed and 10 cm in diameter. The blades protrude 1 cm from the rotor hub. The rotor is about 10 cm high and extends the full depth of the vessel.

to maintain network disruption with the consequent dissipation of energy. At medium mass concentrations, the solidlike properties of the suspension often required that motion be attained using positive-displacement types of pumps and mixers. In the early 1980s, Gullichsen and Harkonen (1981) showed that medium consistency suspensions behaved in a fluidlike manner provided that sufficient shear was applied to them. This corresponded to the onset of a turbulent flow regime. This led to development of centrifugal medium consistency devices, including mixers and pumps.

A typical plot of torque (shear stress) versus impeller rotational speed (shear rate) for a medium consistency pulp suspension is compared with that of water in Figure 20-8. The device used for the test had Couette geometry, with baffles on the vessel wall to prevent solid/suspension slip at the vessel periphery. For water, torque increased with the square of rotational speed, as expected for a Newtonian fluid mixed under turbulent conditions. For the pulp suspension, a significant torque was measured before rotation began. This was due to the network strength. Once the suspension yielded, a slip plane was created in the suspension immediately adjacent to the rotor. The torque fell dramatically. Increasing the rotor speed enlarged the region of active suspension motion as more and more flocs were entrained in the flow (illustrated in the inset to Figure 20-8). The flow followed streamlines around the rotor, and individual fiber flocs were observed in the flow. The torque increased as more suspension was brought into motion. When the flow reached the vessel wall, a transition to turbulence began. At this point (marked by a solid point on the graph), all suspension was in motion and the yield stress was exceeded everywhere in the vessel. Creation of this fluidized

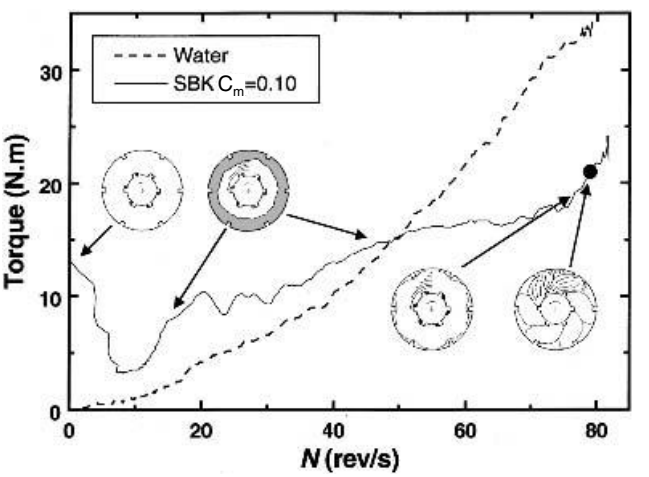

Figure 20-8 Torque versus impeller speed for water and a $C_m = 0.10$ bleached kraft suspension measured in the Couette test apparatus described in the caption to Figure 20-7. The insert diagrams show the observed pulp suspension motion at points along the flow curve.

or fluidlike state became one criterion used in the design of these processing devices. Although individual flocs could be seen in the flow, they were dispersed as they moved into the rotor vicinity (Bennington, 1988).

The onset of fluidization marks the beginning of the transition to turbulence and is device dependent. This transition was studied under operating conditions typical of medium consistency pumps and mixers (Bennington et al., 1991; Bennington and Kerekes, 1996). The average energy dissipation measured at the onset of turbulence, ε_F (in W/m^3), was correlated by the equation

$$\varepsilon_F = 4.1 \times 10^9 C_m^{2.5} (D/T)^{2.3} \tag{20-19}$$

where T is the housing (mixer) diameter, D the rotor diameter, and C_m is expressed as a fraction. In the limit that $D/T \rightarrow 1$, a device-independent estimate of the power required to initiate turbulence in a pulp suspension was obtained. Industrial equipment usually operates at average dissipation levels lower than this value.

The measurement of the transition to turbulence and its comparison with power curves developed in the same device using Newtonian fluids allows the apparent suspension viscosity to be estimated. For medium consistency suspensions, the apparent viscosity is high. For example, for an FBK at $C_m = 0.10$, μ_a is approximately 2 Pa · s at the fluidization point (Bennington and Kerekes, 1996).

20-3.5 Turbulence Suppression in Pulp Suspensions

Creation of turbulence in pulp suspensions is needed to disperse fiber aggregates and to augment mass transfer within the suspension. Disruption of the fiber network requires considerable energy, and the fibers themselves modify the turbulence within the suspension. Experimental measurements for pulp suspensions have been limited to suspensions at low concentration due to interference between the fibers and invasive probes, or due to attenuation of optical signals by suspension opacity. Most studies have concluded that fibers suppress turbulence within the suspension, although some have reported turbulence enhancement. The studies indicate complex interaction between the fibers, fiber flocs, and the flow (Bennington and Mmbaga, 1996).

Mixing-sensitive chemical reactions have been used to probe liquid-phase turbulence within pulp suspensions (Bennington and Bourne, 1990; Bennington and Thangavel, 1993; Bennington and Mmbaga, 2001). As with previous studies, pulp fibers were found to attenuate liquid-phase turbulence under most mixing conditions. This was attributed to dissipation of energy by friction at fiber–fiber contact points. Under certain conditions, the local energy dissipation was slightly increased, probably due to local redistribution of energy within the mixer. Mapping this dissipation in a typical high-shear mixer showed modification of its distribution throughout the vessel volume when compared with water (Figure 20-9). However, the liquid-phase energy dissipation decreased exponentially with increasing suspension concentration.

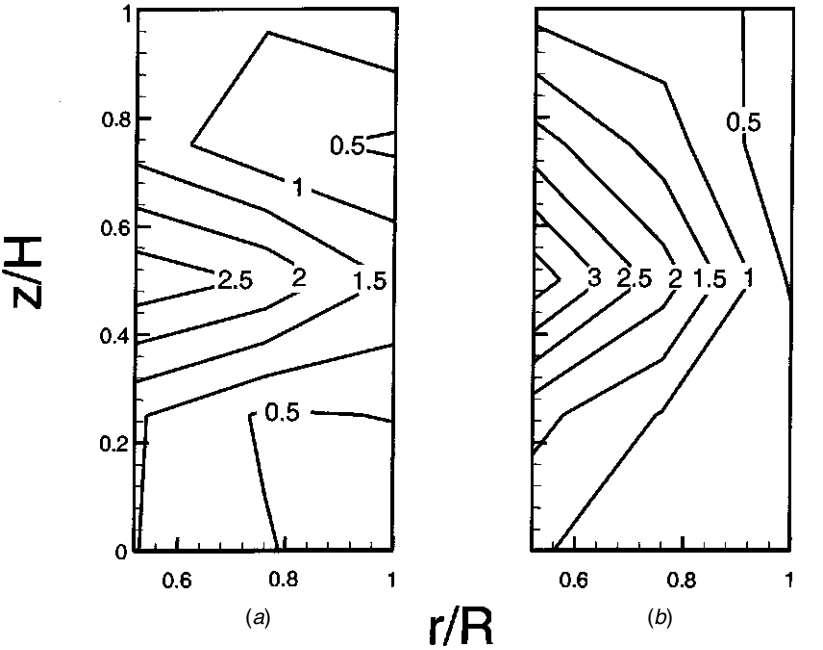

Figure 20-9 Two dimensional map of the normalized local energy dissipation ($\varepsilon_{loc}/\varepsilon_{avg}$) measured in a plane midway between wall baffles in a medium-intensity mixer. The mixer is a concentric-cylinder device having a depth of 10 cm and a diameter of 19 cm. Four 1 cm baffles are spaced at 90° intervals around the vessel periphery. The rotor is four-bladed, 10 cm in diameter, with the blades protruding 2.5 cm from the rotor hub. The input (ε_{in}) and average (ε_{avg}) (measured) energy dissipations are given for two cases: (*a*) water ($\varepsilon_{in} = 101 \pm 5$ W/kg, $\varepsilon_{avg} = 120 \pm 13$ W/kg) and (*b*) a $C_m = 0.013$ FBK pulp suspension ($\varepsilon_{in} = 101 \pm 5$ W/kg, $\varepsilon_{avg} = 33 \pm 5$ W/kg). Note that the distribution map gives the local energy dissipation in the liquid phase only. Energy dissipated by the fibers is not measured. Tests were made at N = 17.3 rps.

20-3.6 Gas in Suspension

Gas is often present in pulp suspensions, reaching significant volumes in the medium consistency range (Dosch et al., 1986). For example, for a $C_m = 0.10$ kraft pulp, gas can occupy 10 to 20% of the suspension volume. This gas is readily separated from the suspension when subjected to centrifugal fields, such as those created by pumps and mixers. This provides a method of removing gas from suspensions (using centrifugal pumps) but creates difficulties when gases must be mixed into them. Gas, when present, can reduce the effective suspension density in the impeller vicinity, reducing both motion and energy dissipation in the suspension. This results in reduced gas–liquid mass transfer. Even when the gas volume in the suspension is small, gas can accumulate and be held up within the mixer.

The efficiency of gas mixing can be evaluated by measuring the rate of mass transfer from the gas to the liquid phase. This has been done in the laboratory using high-shear mixers similar to those used in industry (Bennington et al., 1997a; Rewatkar and Bennington, 2000). For an FBK fiber suspension in batch operation, the volumetric gas–liquid mass transfer coefficient, k_La, was correlated with power dissipation per unit volume, ε_v, the gas void fraction in the mixer, ϕ_g, and the suspension mass concentration (as a fraction), C_m. This gave

$$k_La = 1.17 \times 10^{-4}\varepsilon_v^{1.0}\phi_g^{2.6}\exp(-38.6C_m) \tag{20-20}$$

Ninety-five percent confidence intervals were determined for each fitted parameter. For power dissipation this was 1.0 ± 0.38, for void fraction 2.6 ± 0.65, and for mass concentration -38.6 ± 11.0. The dependence of k_La on power per unit volume is higher than that reported by other investigators, which typically have exponents ranging from 0.4 to 0.8 (Mann, 1983; Tatterson, 1991). Further, the dependence of k_La on the gas void fraction is significantly higher than found in stirred vessels, where proportionality is expected. Increasing the suspension mass concentration exponentially reduces gas–liquid mass transfer, with the reduction (compared with water) being an order of magnitude for a $C_m = 0.10$ suspension. This is shown in Figure 20-10, where k_La values measured for a representative set of operating conditions are plotted against suspension volume concentration. The reduction in k_La parallels the reduction in liquid-phase turbulence measured in the suspension (Mmbaga, 1999; Rewatkar and Bennington, 2000).

Gas–liquid mass transfer can dramatically affect certain bleaching reactions. For rapid reactions such as delignification with ozone, the rate of ozone mass

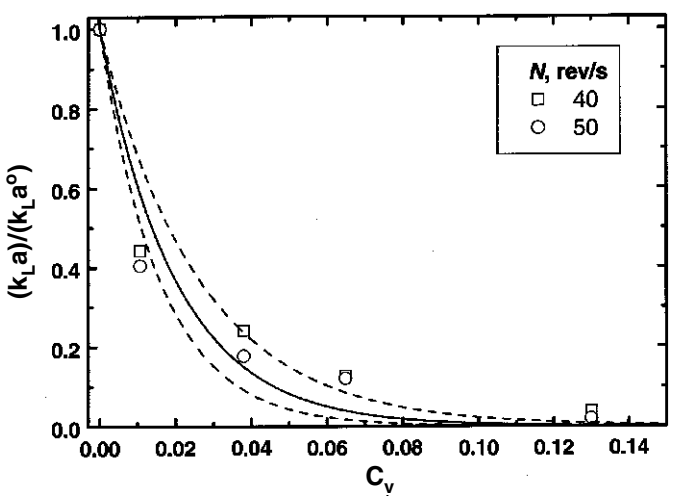

Figure 20-10 Relative volumetric gas–liquid mass transfer coefficient (k_La) versus suspension volumetric concentration for tests made in a high-shear laboratory mixer. Tests were made in a commercial laboratory pulp mixer (Quantum MK-IV).

transfer determines the effective reaction rate. Here, the extent of bleaching is determined by mass transfer achieved in the mixer (Bennington et al., 1997a).

20-4 SCALES OF MIXING IN PULP SUSPENSIONS

Mixing is often targeted at a particular scale, depending on the purpose of mixing (reaction, blending, etc.). In a liquid, mixing scales are determined by the scale of turbulence generated within them. In a pulp suspension, mixing scales are imposed by the fiber dimensions. A fiber scale can be defined as having dimensions between that of a fiber diameter and a floc length (typically, two to three fiber lengths). The macroscale encompasses scales larger than the floc dimension and the microscale encompasses scales below a fiber diameter, as summarized in Table 20-1.

As engineers, we often think of scales associated with processing equipment: the volume of a tank or mixer, the diameter of a section of piping, and so on. In many situations, a satisfactory process outcome also requires that good fiber scale and/or microscale mixing be attained. Accomplishing the required mixing and uniformity in a pulp suspension can be more difficult than in fluid systems due to the suspension rheology.

20-5 MACROSCALE MIXING/PULP BLENDING OPERATIONS

20-5.1 Homogenization and Blending

The agitation of pulp stock for homogenization and blending is the most common mixing operation in pulp and paper manufacture. The blend chest (a "well-mixed" stirred vessel) illustrates the importance of macroscale mixing in pulp and paper processes. It is the heart of the stock preparation system and is used to mix two or more pulp streams, often with wet-end chemicals, dyes, fillers or additives, as well as providing a uniform feed of stock to the paper machine. Mixing chests

Table 20-1 Mixing Scales in Pulp Suspensions

Mixing Scale	Scale Dimension Size (cm) [Volume (cm^3)][a]	Mixing Achieved by:	Physical Scale
Macroscale	>1.0 [0.5]	Bulk motion	Tanks, pipes, vessels
Fiber scale	0.005–1.0 [7×10^{-8}–0.5]	Laminar and turbulent shear, diffusion	Fibers and flocs
Microscale	<0.005 [7×10^{-8}]	Diffusion aided by small scale fluid motion	Fiber diameter and fiber wall thickness

[a] Assuming spherical geometry.

act as low-pass filters and ensure uniform mass flow ahead of many downstream operations in addition to the paper machine, including bleaching stages, washers, screens, and cleaners. In most cases, process control strategies are used to deal with long-term consistency fluctuations.

The economics of less-than-perfect macroscale mixing are difficult to assess, although an estimate can be made. From studies of paper machine variability, Bialkowski (1992) found that 55% of the variability in final paper quality was at frequencies due to flow instabilities and mixing deficiencies. These frequencies were higher than could be removed by process control strategies. It is difficult to relate paper machine efficiency (breaks, etc.) to this process variability. However, if we assume that the process variability is directly related to machine downtime, the economic impact of mixing nonuniformity can be estimated. Paper machine lost time averages approximately $10 000 per hour, and the total yearly operating efficiency of a paper machine is around 80 to 95% (personal communication, Pikulik, 2001). If only 1% of operating efficiency is lost due to mixing related inefficiencies, the cost for the average paper machine would be $800 000 per year! Other estimates have been made for improved consistency control and have yielded savings of similar magnitude (Jansson, 1999).

Another example of the importance of good macroscale mixing of pulp suspensions is consistency control ahead of a bleaching stage. Poor mixing can result in the over-or under-application of bleaching chemicals on pulp, which can impair pulp quality as well as increase chemical costs. A typical bleaching response is nonlinear, with increasing amounts of chemical required to obtain an increased bleaching response. If consistency control is poor ahead of a bleaching operation, some pulp must be overtreated to compensate for the periodic episodes of higher mass flow (a high consistency excursion). Because the frequencies of these disturbances are higher than can be eliminated by either feedforward or feedback control, overcharging is the only alternative to better mixing. Typically, the standard deviation of consistency measurement is 3 to 5% (Jansson, 1999). The increased chemical required to compensate for poor consistency control can be substantial and adds to the cost of bleaching the pulp. Just reducing the standard deviation from 5% to 3% (which could be done by measuring the consistency with a more accurate consistency meter) was estimated to be worth $250 000 per year in one chlorine dioxide bleaching application (Jansson, 1999). Further, the variability in fiber treatment can be propagated down the fiber line, affecting succeeding stages and contributing to nonoptimal strength delivery from the bleaching system.

The design of stock chests is concerned largely with selecting the power necessary to ensure complete motion throughout the chest volume. The impeller power for suspension agitation has been correlated with the apparent viscosity of the suspension, assuming Bingham plastic behavior. Thus,

$$\mu_a = \frac{\tau_y + \mu_p \gamma}{\gamma} \tag{20-21}$$

where τ_y is the yield stress of the suspension, μ_p the plastic viscosity, and γ (du/dy) the shear stress. Using the Metzner–Otto correlation and assuming that

the plastic viscosity is close to that of water (and thus an insignificant contribution to the apparent viscosity compared with the yield stress), the apparent viscosity can be expressed as

$$\mu_a = \frac{\tau_y}{10N} \tag{20-22}$$

which can then be used in calculation of the impeller Reynolds number. In practice, suspension behavior has been correlated with a stock parameter m (often used in correlations or to form a modified Reynolds number), given by

$$m = \sqrt{\frac{\tau_y}{\rho}} \tag{20-23}$$

The parameter m must be determined for each pulp stock [essentially by measuring the suspension yield stress, which is affected by many suspension parameters; see eq. (20-17)]. Correlations made using this procedure allow the behavior of different stocks to be correlated and for differences in impeller type and location to be expressed (Blasinski and Rzyski, 1972).

Gibbon and Attwood (1962) addressed the issue of scaling chest design, finding that impeller power scaled as

$$\frac{P_1}{P_2} = \left(\frac{D_1}{D_2}\right)^{2.75} \tag{20-24}$$

for equal process flow in geometrically identical chests. Here P is the impeller power and D the impeller diameter for chests 1 and 2. The measured scaling dependence of 2.75 lies between that of constant power per unit volume [one common method used for scaling pulp chest volume (an exponent of 3.0)] and that of constant tip speed (an exponent of 2.0). One still must measure the power consumption needed for adequate mixing at one chest scale. This is usually assessed visually as a condition of complete active suspension motion on the chest surface, which at best is a subjective measure. In addition, stagnant regions can exist below the suspension surface in vessel corners, as observed in a Plexiglas laboratory scale chest (Ein Mozaffari et al., 2001).

The dynamics of pulp chests in pulp processes have been modeled assuming ideal mixing and first-order behavior (Walker and Cholette, 1958; Reynolds et al., 1964). This allows chest design (essentially the chest volume) to be based on the anticipated disturbances and degree of attenuation required. However, these studies did not include allowances for nonideal suspension flow that can create bypassed regions and dead zones in the chest.

Industrial chests are known to behave nonideally. The response of a typical rectangular blend chest (L : W : D = 6.1 : 4.6 : 4.3 m, volume = 120 m^3) to a step change in consistency is shown in Figure 20-11. Based on these data, the Bode plot of the chest was constructed as shown in Figure 20-12. Significant departure from ideal behavior (the dashed curve) was measured between frequencies of

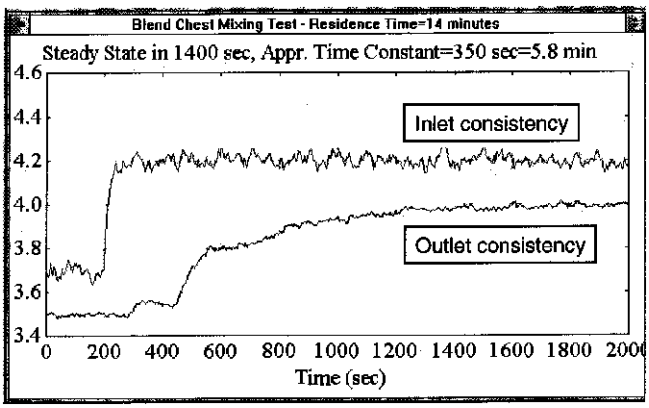

Figure 20-11 Response of an industrial stock chest to a step change in mass concentration at t = 200 s. The mass concentration (in percent) is given on the y-axis.

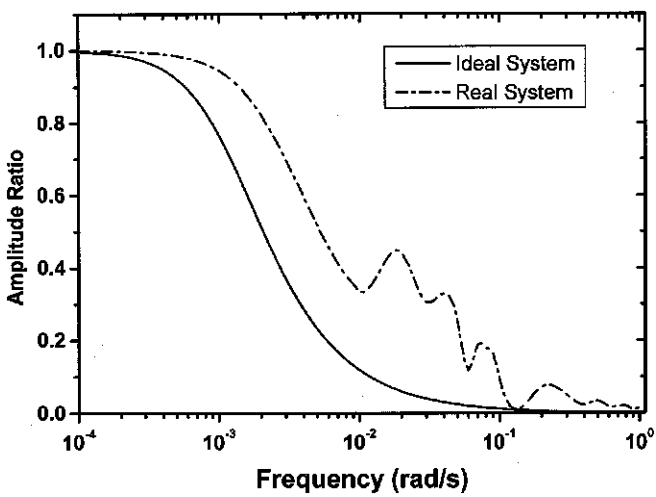

Figure 20-12 Bode plot showing the amplitude ratio versus disturbance frequency for an industrial chest (Figure 20-11) and an ideal mixed chest of the same volume.

0.01 and 0.1 rad/s. This leads to problems in uniformity that cannot be removed by control strategies.

Currently, industrial chest design is based largely on proprietary criteria developed from accumulated experience (Oldshue, 1983; Yackel, 1998). One method uses the momentum required to agitate pulp stock within a chest. The momentum needed for surface motion of the pulp suspension has been correlated with a range of design variables, including the chest size and geometry, impeller location(s), the type of fiber and suspension mass concentration, and the desired retention time. Based on the required momentum, an appropriate impeller is selected. A

similar approach is followed when designing limited agitation zones in larger vessels: for example, a low consistency extraction zone in a high-density pulp storage tower. These procedures are not linked directly to suspension rheology, although suspension rheology certainly dictated the correlations. Adjustments can be made depending on the pulp type used (through factors). However, these design procedures provide no indication of the degree of motion generated in the suspension. (Indeed, the original data upon which the correlations were developed are not given.)

Computational fluid dynamics permits solution of the entire suspension flow field, although considerable computer power is needed. CFD has been applied to pulp suspension agitation by Bakker and Fasano (1993), who treated the pulp suspension as a Bingham fluid. Calculations were first performed assuming turbulent flow. The turbulent shear rate was then compared with the shear rate required to disrupt the fiber network. If the shear was insufficient, calculations were redone for laminar flow. Calculated suspension velocities of less than 0.001 m/s were treated as being stationary. The simulation solutions corresponded to visual observations made in a laboratory chest, although the size of the agitated region was underpredicted. Turbulent motion was often limited to the immediate vicinity of the impeller.

Clearly, more work needs to be done in the area of macroscale mixing of fiber suspensions. Links are needed between suspension rheology, the desired process outcome (i.e., degree of suspension motion), and the chest design. The ability to design a blending system with known process dynamics is needed. This would also enable the synergism between process control and mixing to be fully exploited.

Pulp processing devices are also used to mix and simultaneously produce physical changes to the pulp. One example of this is in repulping operations.

20-5.2 Repulping

The repulping or reslushing of paper is an integral part of paper manufacture. *Broke and trim*, paper produced but not wound onto the reel, must be repulped and returned to the machine for reprocessing. In paper recycling, postconsumer paper products (often, old newspapers and old magazines) are the main source of recycled fiber. These must be repulped to liberate the individual fibers, and ink and other contaminants must be detached from the fiber surface and separated from the suspension. Repulpers must also blend the paper furnish thoroughly and mix chemicals and additives into the pulp.

Repulpers can be of a number of designs. Figure 20-13 shows a laboratory pulper modeled after a common industrial design. The repulper uses a triple-flighted helical rotor, a conical tub, and wall baffles to ensure complete motion in medium consistency suspensions. The laboratory unit operates on a batch size of 8 kg of pulp. Industrial units have volumes up to 160 m^3. Despite this disparity in size, the progress of deflaking and ink detachment can be modeled using a mixing-controlled mechanism based on the force transmitted to the fiber

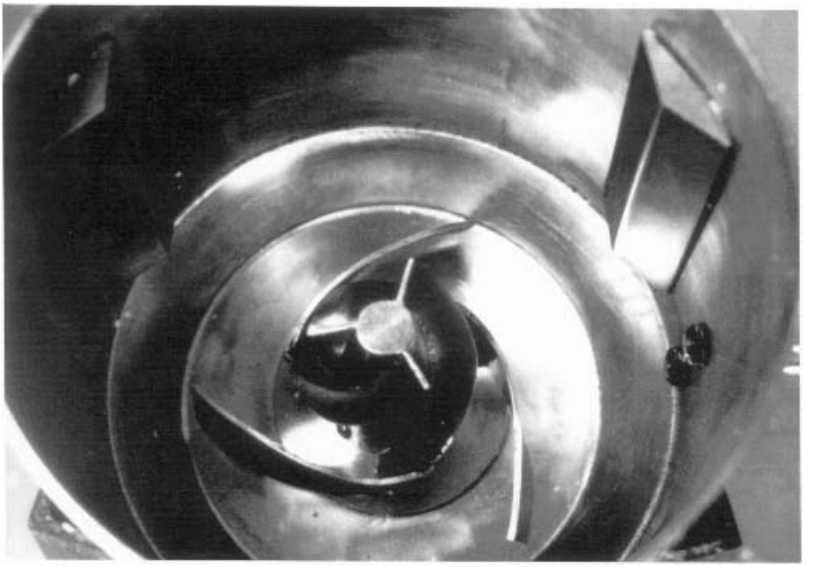

Figure 20-13 Photograph of the laboratory repulper showing the three-vaned helical rotor and wall baffles. The repulper tub has an inner diameter of 30 cm and a working volume of 8 L.

surface by the rotor (Bennington et al., 1998a; Bennington, 1999; Bennington and Wang, 2001).

If deflaking and ink detachment are caused by direct suspension–rotor interaction, the extent of deflaking should be proportional to the extent of this interaction. For a repulper where complete motion exists throughout the suspension, the rate of deflaking is given by the first-order expression

$$\frac{dF}{dC_R} = kF \tag{20-25}$$

where F is the Tappi flake content (the mass of paper flakes retained on a 10-mesh screen following screening), k the rate constant (negative, as the flake content decreases during processing), and C_R the contact area created between the fiber suspension and the rotor. C_R is given by

$$C_R = SC_v \tag{20-26}$$

where C_v is the volume concentration of the suspension [see eq. (20-13)] and S is the area swept out by the rotor, given by

$$S = NBGt \tag{20-27}$$

where N is the rotor speed, B the number of rotor vanes, G the surface area that a single rotor vane sweeps out during one revolution, and t the time. G is

calculated knowing the rotor geometry and the height of suspension in contact with the rotor.

The rate of deflaking, k, will depend on two factors: the strength of the material being pulped and the force applied by the rotor to the suspension. Thus,

$$k = k_o \exp\left(-\frac{T_M}{KF_R}\right) \tag{20-28}$$

where k_o is the intrinsic rate constant, T_M the strength of the material (the paper strength in the case of deflaking), F_R the force per unit length of rotor vane, and K a proportionality constant. F_R can be evaluated by measuring the torque on the rotor shaft:

$$F_R = \frac{T}{(D_m/2)BH_C} \tag{20-29}$$

where T is the torque, D_m the average rotor diameter, and H_C the rotor height in contact with suspension. Alternatively, F_R can be evaluated knowing the power number at the given operating conditions.

The use of these equations has allowed a wide range of data to be explained, as illustrated in Figure 20-14. Here a number of recycled paper materials of varying strength (wet-tensile strength) and suspension mass concentration were repulped in a 21 L laboratory repulper. The extent of flake removal is plotted against kC_R, which accounts for equipment geometry, operating conditions, and paper strength. Within experimental error, the data agree. This supports the interpretation of

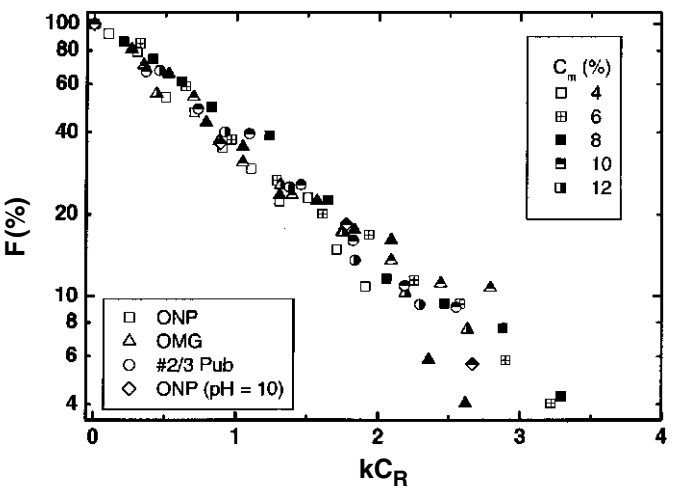

Figure 20-14 Tappi flake content versus fiber–rotor contact area (C_R) [see eq. (20-25)] for four different recovered paper furnishes. The suspension mass concentration and paper type are parameters. ONP, OMG, and #2/3 PUB are old newspaper, old magazine, and a high-grade publishing furnish, respectively.

deflaking as being caused by physical interaction between the paper and the rotor. The model has been verified for varying rotor speeds and rotor designs, has been used successfully in the mill, and can be modified for different mass contents in the repulper (Bennington et al., 1998b).

Ink detachment is more difficult to model than deflaking. Ink is attached to fiber with a certain adhesive force. If this attachment force is greater than the force applied by the rotor, the ink will remain attached to the fiber. Ink can also be hidden in fiber interstices, and thus not be subjected to the rotor forces. Both these factors contribute to a floor level of ink that remains following repulping. Further, ink can be redeposited onto or inside the fiber once it has been detached from the fiber surface. The latter phenomenon, called *lumen loading*, is a function of mixing action, which increases with ink concentration and the duration and intensity of suspension treatment.

If one considers these factors, the observed detachment behavior can be modeled in a manner analogous to deflaking. This gives the ink concentration remaining on the fiber as a function of time, $C_I(t)$:

$$C_I(t) = C_I^f + (C_I^o - C_I^f)e^{k_I t} + k_R \int_{t=o}^{t} (C_I^o - C_I(t))\, dt \qquad (20\text{-}30)$$

where C_I^f is the floor level of ink that cannot be removed and C_I^o is the initial ink concentration. k_I is the rate constant (again negative) for ink detachment, which can be expressed by an equation analogous to that of eq. (20-28). k_R (positive) is the rate of ink redeposition, which can be measured experimentally. Thus, the ink concentration remaining on the fiber at any time depends on three factors: the ink that cannot be removed, the ink that can be removed (with ink removal following first-order kinetics similar to that for deflaking), and the amount of ink redeposited on the fiber (Bennington and Wang, 2001).

20-5.3 Lumen Loading

Most of the ink irreversibly redeposited in recycling operations is deposited inside the fiber lumen (Ben and Dorris, 1999) with the extent of redeposition affected by the mixing action imparted during suspension processing (Bennington and Wang, 2001). Lumen loading of ink is undesirable, as it cannot be removed subsequently. However, lumen loading can be used to enhance certain sheet properties. In papermaking, it is often desirable to load the sheet with filler materials to enhance their optical properties. However, filler that remains on exterior fiber surfaces interferes with bonding and reduces the physical strength properties of the paper. Processes to load the filler inside the fiber lumen allow the benefits of increased filler levels to be realized without compromising the strength properties of the sheet. Lumen loading is facilitated by the high-shear mixing of pulp in an excess of filler material. As shear increases, so does the level of mechanical action. This causes more filler to enter and remain in the lumen (Middleton and Scallan, 1993). No commercial application for intentional lumen loading of pulp fibers is currently operated.

20-6 MIXING IN PULP BLEACHING OPERATIONS

20-6.1 Pulp Bleaching Process

Pulp bleaching selectively removes unwanted components (chromophores) from the fiber wall using a series of increasingly selective chemicals and reaction conditions. One common bleaching sequence used to produce fully bleached kraft pulp is the OD(EO)DED sequence. (Each letter represents a distinct chemical used in a separate bleaching operation or stage). Typical reaction conditions for each stage in this sequence are given in Table 20-2, although conditions vary from mill to mill [see individual chapters in Dence and Reeve (1996)]. Other bleaching sequences and bleaching chemicals can also be used. For example, peroxide and ozone are increasingly incorporated in bleaching sequences, alone or in conjunction with other chemicals.

Bleaching reactions are complex, with many different chemical species involved in any given reaction. For example, hundreds of chlorinated products have been identified in extracts made from pulps bleached in a number of chlorinated sequences (Reeve and McKague, 1990). Although model compound studies are useful for elucidating chemical reactions and reaction mechanisms, the majority of bleaching studies measure an averaged bleaching response over all targeted compounds. As bleaching involves lignin removal (a heterogeneous polymer with a multitude of chemical structures and reactive sites) it is common to represent its removal using standardized tests. The kappa number (the percent lignin is approximately equal to 0.15 times the kappa number) is commonly used for this purpose (Tappi Test Methods, T236 cm-85). At low lignin concentrations (<0.5%) the kappa test is not accurate. Here, the progress of the bleaching reaction can be followed using brightness development (Tappi Test Methods, T452 om-98).

Table 20-2 Typical Conditions for Bleaching Reactions: OD(EO)DED Sequence

	Stage Reaction Conditions						
Stage Designation	Suspension Concentration (C_m)	Chemical	Chemical Charge (kg/t)	Reaction Temperature (°C)	System pH	System Pressure[a] (kPa)	Residence Time (h)
O	0.08–0.14	O_2	20–30	85–100	10–12	140–660	0.5–1.5
		NaOH	25–30				
		M_gSO_4	0–2.5				
D	0.03–0.04	ClO_2	15	30–60	1.5–3	100	0.3–1.0
EO	0.10–0.12	NaOH	25	70	10.5	100–300	1.0
		O_2	5				
D	0.10–0.12	ClO_2	8	70	3.5	100	2.0
		NaOH	5				
E	0.10–0.12	NaOH	5	70	10.5	100	1.0
D	0.10–0.12	ClO_2	5	70	4	100	3–5

Source: Based on data taken from Dence and Reeve (1996) and other sources.

[a] At top of tower. Pressure at the tower bottom will have hydrostatic head added, typically 300 kPa.

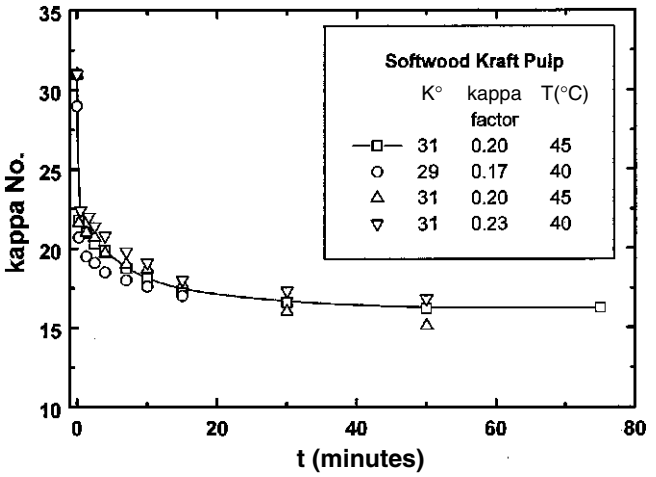

(*a*)

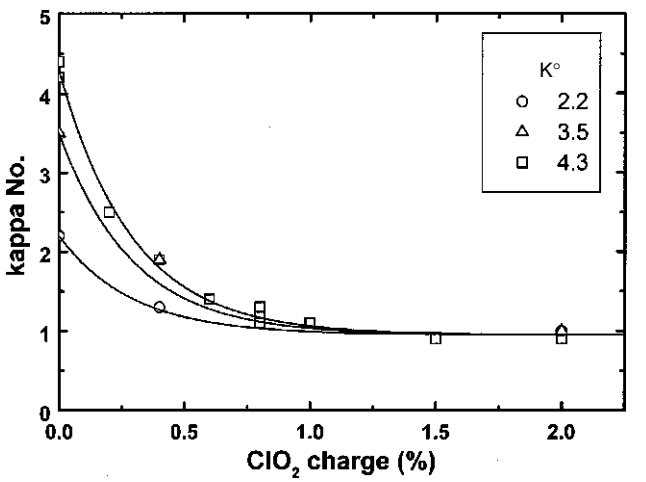

(*b*)

Figure 20-15 Typical pulp bleaching results. (*a*) Kappa number versus reaction time for chlorine dioxide (D_0) delignification of a softwood kraft pulp ($C_m = 0.031$, initial pH ~ 3). (From Tessier and Savoie, 1997.) (*b*) Kappa number following chlorine dioxide (D_1) bleaching of a kraft softwood pulp. Pulp was bleached in the mill using a DE_{OP} sequence and laboratory bleached (D_1) with hand mixing (at $C_m = 0.10$ and $T = 74°C$). (From Bennington et al., 2001.)

The progress of a typical bleaching reaction is illustrated in Figure 20-15. In Figure 20-15*a*, the reduction in kappa number is plotted against time for delignification with chlorine dioxide in the first delignification stage (D_0). The initial chemical reaction is rapid and the majority of the bleaching response occurs during it. The rapid reaction is followed by a falling-rate period, where reaction

slows and eventually tapers off. This leaves residual lignin in the fiber. Increasing the chemical charge increases lignin removal (as shown for chlorine dioxide delignification in Figure 20-15*b*), but it is difficult to achieve complete removal in a single stage. The aggressive conditions required to delignify pulp completely in a single stage would impair pulp strength. Consequently, the residual lignin must be reactivated (using an extraction stage, for example) and removed in subsequent bleaching stages. All bleaching reactions display these characteristic attributes, which are reflected in the design of the typical bleaching stage, illustrated in Figure 20-16.

In a typical bleaching stage, pulp from the previous stage is washed to remove reacted and dissolved substances leached into the process liquor. The pulp is then prepared for reaction. Steam is used to raise the pulp to the reaction temperature and the process pH set. The bleaching chemical is then added, usually in a dedicated mixer, and the suspension passed into a tower for a period to ensure bleaching reaches completion. This time varies widely. For ozone delignification, it can be as short as 1 min. For chlorine dioxide brightening, it can be as long as 5 h. The pulp is then washed before being sent for further processing.

20-6.1.1 Mixing and Chemical Reaction. Lignin and cellulose are contained within the fiber wall. The selectivity of a bleaching process (usually defined as the ratio of lignin removal to a measure of the concurrent damage to cellulose) is controlled primarily by the reaction chemistry and processing conditions (chemical charge, suspension mass concentration, temperature, pH). The extent of reaction (determined by chemical dosage and reaction time) can

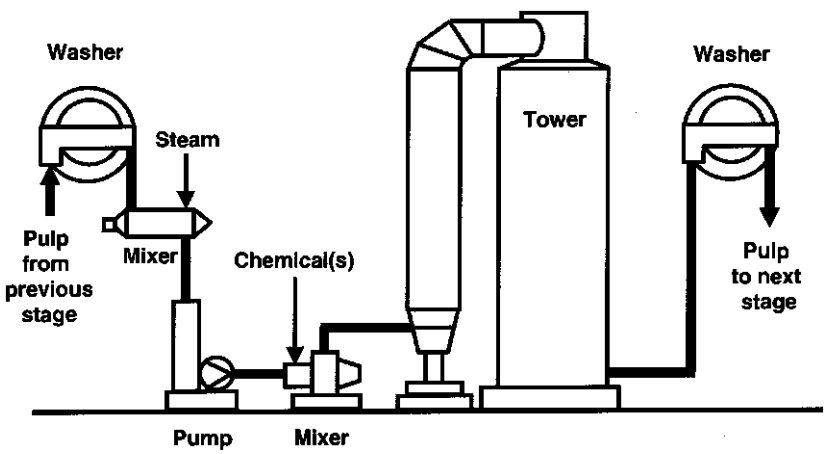

Figure 20-16 A bleaching stage consists of prewashing, mixing for steam addition (temperature adjustment), mixing for chemical addition, pulp retention in a tower, and postwashing. The diagram is typical of a chlorine dioxide bleaching stage (D_1 or D_2) and shows only the pulp and chemical flows. Filtrate flows are not shown.

also be controlled to minimize pulp damage. Controlling these parameters permits the optimization of bleaching and pulp strength over an entire bleaching process.

In pulp passage through a mixer it is desirable to disrupt the fiber network (break apart the individual flocs) and commingle each fiber with the appropriate amount of bleaching chemical. Many mixers are designed to achieve this dispersed state. On exiting the mixer, the suspension rapidly reflocculates (for a $C_m = 0.10$ suspension in as little as 10^{-4} to 10^{-3} s). From this point onward, the reaction can be viewed as continuing in tiny individual reactors (the flocs) as they are conveyed through the remainder of the bleaching stage. Within the flocs, diffusion plays a large role in bringing chemical to regions where it is consumed. As the mixing quality attained on exiting the mixer can be essentially "locked in" for the remainder of the bleaching stage, mixture quality at the mixer exit must be good. Further, the rate at which this mixing occurs must be rapid compared with the net chemical reaction rate, or bleaching will occur under nonhomogeneous conditions.

As in aqueous systems, characteristic times for mixing (τ_M) and chemical reaction (τ_R) can be calculated and compared to determine whether mixing rate influences the outcome of a bleaching reaction. In the instantaneous ($\tau_M \gg \tau_R$) and fast regimes ($\tau_M \simeq \tau_R$), reaction occurs more rapidly, or at the same rate, as mixing. Here mixing can affect reaction. In the slow regime ($\tau_M \ll \tau_R$), mixing is complete before reaction begins and chemical kinetics govern the reaction outcome. As mixing occurs on a continuum of scales, time constants at appropriate scales must be compared with the bleaching reaction rate to see if mixing is important at that scale.

Mixing and reaction time constants are not readily calculated for pulp suspensions. Mixing rate is influenced by the complex suspension rheology. Bleaching rate is influenced by chemical diffusion into the fiber wall and can be controlled by mass transfer. Further, in laboratory experiments a net reaction rate is measured and may have been influenced by the mixing conditions during the test. Despite these concerns, a number of estimates can be made.

Mixing time constants can be estimated at a number of scales based on mixer design and operating conditions, chemical contacting strategy, and the level of turbulence generated in the suspension. A macroscale time constant may be based on the process time (the total residence time in the bleaching stage) or the mixer residence time. None of these time constants addresses the quality of mixing attained, which is discussed later.

The location of chemical injection may also be important for the bleaching reaction. Mesomixing time constants can be expressed as the characteristic time for turbulent dispersion of the chemical feed stream or for disintegration of large eddies into smaller ones. A number of methods for estimating these are given by Baldyga and Bourne (1999), and one can define others for fibrous suspensions. For example, the time required for dispersion of a floc could be used as a mesomixing time.

At the smallest scales, a micromixing time constant can be given by the reciprocal of the engulfment rate during mixing, τ_E. This is given (Baldyga and

Bourne, 1989) as

$$\tau_E = 12.7\left(\frac{\nu}{\varepsilon}\right)^{0.5} \tag{20-31}$$

The kinematic viscosity of suspension, ν, can be estimated using an approximation suggested by Bennington and Kerekes (1996):

$$\nu = \frac{\tau_y^2}{\varepsilon\rho^2} \tag{20-32}$$

where ε is the energy dissipation in W/kg and ρ is the suspension density. The suspension yield stress can be estimated by an appropriate correlation. For a semibleached kraft pulp, for example, the yield stress was correlated using (Bennington et al., 1990)

$$\tau_y = 3.2 \times 10^6 C_m^{2.8} \tag{20-33}$$

where τ_y is in Pascal and C_m is expressed as a fraction.

Estimates for mixing time constants are given in Table 20-3 for typical bleach mixers. Two estimates are made for τ_M: the process mixing time constant, τ_P (assuming a 90% reduction in the incoming variability by a first-order process) and the micromixing time constant, τ_E [calculated using eqs. (20-31)–(20-33)].

Bleaching chemicals react with dissolved substances in the process liquor, and with chemical species both on the fiber surface and within the fiber walls. For reaction with compounds dissolved in the process liquor or located on the fiber surface, appropriate time constants can be estimated from model compound studies conducted in the aqueous phase. However, most bleaching studies measure a net or aggregate bleaching rate with the pulp.

This bleaching rate is determined by the bleaching chemical used and its form (liquid or gas), the nature of the target compounds (usually, a wide range of

Table 20-3 Time Constants for Mixing in Pulp Bleaching Operations

Mixing Conditions				Mixing Time Constants	
Mixer	C_m	Energy Dissipation, ε (W/kg)	Mixer Residence Time (s)	τ_P (s)	τ_E (s)
Hand mixing	0.03	20	30	13	0.43
	0.10	50	30	13	5.0
Stirred tank	0.03	0.4	300	130	21.3
Static mixer	0.03	30	4	1.7	0.3
Peg mixer	0.10	100	10	4.3	2.5
High-shear	0.03	4000	0.3	0.1	0.002
	0.10	4000	1	0.4	0.06

similar compounds), and their location in the suspension. Compounds dissolved in the liquid phase are readily accessible to the bleaching chemical. However, the target compounds are located within the fiber wall and diffusion may control the reaction rate. Reaction progress is followed using an aggregate measure of the compounds, including the kappa number (lignin content), brightness development (chromophore removal), or pulp viscosity (cellulose depolymerization or degradation). Further, bleaching studies (like those of Figure 20-15) are influenced by laboratory mixing conditions (and are often not characterized).

A range of kinetic expressions is reported in the literature for common bleaching chemistries (see, e.g., Dence and Reeve, 1996; Gullichsen and Fogelholm, 1999). The net bleaching rate can often be approximated by first-order kinetics over industrially relevant time scales (seconds to minutes); for example, for delignification

$$-\frac{dL}{dt} = k_{eff}[L] \tag{20-34}$$

where L is a measure of lignin content (e.g., the kappa number) and k_{eff} is the effective first-order rate constant. Typically, a rapid (or initial) and slow (or residual) rate constant can be determined for each bleaching reaction. The initial rate of reaction is appropriate for comparison with the rate of mixing. Reaction time constants, τ_R, were given by the relaxation time

$$\tau_R = 1/k_{eff} \tag{20-35}$$

Net reaction time constants were estimated by determining effective first-order rate constants using kinetic data found in the literature (Bennington et al., 1989). Calculated values were $\tau_R = 3.9 - 29$ s for chlorination, $\tau_R = 280$ s for delignification with chlorine dioxide, and $\tau_R = 1100$ s for caustic extraction (these include any mass transfer resistance in the system). If we compare these reaction time constants with the mixing time constants given in Table 20-3, we see that in most cases chemical reaction controls the bleaching outcome (i.e., $\tau_M < \tau_R$). Some exceptions are apparent and may explain past trends in mixer selection. For example, the industry moved away from using stirred vessels for pulp chlorination service in the 1960s. The unfavorable rate of mixing provided by the stirred tank reactors may have accounted for the shift toward in-line dynamic and static mixers in this application.

Mills are currently presented with the choice of using either high-shear or static mixers for low consistency delignification in the first bleaching stage (usually, with chlorine dioxide or with mixtures of chlorine dioxide and chlorine). In both cases, mixing is sufficiently rapid that either strategy can be used successfully.

High intensity mixers are now commonly used for chlorine dioxide brightening (D_1 and D_2) operations. Indeed, their introduction in the 1980s allowed bleaching efficiency achieved in the mill to meet or surpass that measured in laboratory studies. The high rate of mixing achieved by these mixers probably contributed to this success. However, this is not the complete story. Peg-type mixers are often found in D_1 and D_2 service and have $\tau_M < \tau_R$. The use of high-shear

mixers in this application enabled significant chemical savings to be achieved. This is probably due to the low energy dissipation in the peg mixers, which is insufficient to rupture the fiber flocs. Consequently, all fiber is not effectively exposed to chemical, and mixing quality is not as good as is achieved in the high-shear mixers, where energy dissipation is an order of magnitude higher. Thus, the quality of the mixture exiting the mixer is important in bleaching. Retention towers are incorporated into the design of a bleaching stage to permit homogeneity to be attained (over longer time scales) as well as allowing slower bleaching reactions to reach completion.

20-6.1.2 Diffusion and Retention Towers. The importance of contacting every fiber with bleaching chemical can be illustrated by computing a diffusive time constant for a fiber and comparing it with that of a fiber floc. The diffusive rate constant, τ_D, can be expressed as

$$\tau_D = \frac{\alpha a^2}{D} \tag{20-36}$$

where D is the diffusion coefficient, a the appropriate size dimension of the particle, and α a constant determined by the geometry of the system and the criteria of mixedness chosen. D changes with the molecular weight of the diffusing substance. For bleaching chemicals (low-molecular-weight compounds) the chemical diffusion rate through water is a good approximation for the rate through a swollen fiber wall, although tortuosity, which effectively lengthens the diffusion path, has the effect of reducing D.

The time for diffusion (without reaction) to increase the average concentration within a fiber wall to one-half of its ultimate value, with the fiber treated as a fully collapsed slab of thickness equal to two fiber wall widths, gives $\alpha \simeq 0.19$. For a fiber wall thickness of $a = 4.0 \times 10^{-6}$ m and an effective diffusion coefficient of $D = 1.3 \times 10^{-9}$ m^2/s, $\tau_D = 0.0023$ s. The ozonation of pulp fibers follows a shrinking core mechanism, limited by the rate of ozone diffusion through the fiber wall. Exposed fibers are completely penetrated and reacted in seconds under typical operating conditions (Bennington et al., 1999).

A typical floc has a much longer diffusion path than an individual fiber. For a floc (where $2a \approx 4$ to 10 mm) using the same diffusion coefficient with $\alpha = 0.036$ [for the average concentration of a floc (treated as a sphere) to increase to half of its ultimate value], τ_D becomes 250 s. Tower residence times vary widely depending on the bleaching stage used. The residence time was often determined by the time needed for the bleaching reaction to reach an asymptotic level. These residence times are normally much larger than 250 s (in chlorine dioxide brightening, for example, they can be 3 to 5 h in duration). However, the ability of the retention tower to create homogeneity throughout the fiber suspension must be questioned.

The diffusion distance within fiber suspensions has been measured by several investigators. From an infinite reservoir of reacting chemical, diffusion/reaction distances of 3 to 6 mm were covered in 1 h at $C_m = 0.03$ and distances of 1

to 2 mm at $C_m = 0.10$ (Paterson and Kerekes, 1984). Similar results were found by Bennington (1988), who measured a diffusion distance of 5 mm for a nonreactive tracer through a $C_m = 0.03$ pulp suspension. However, diffusion distances are much shorter under typical bleaching conditions. Here, only a limited quantity of chemical is available for diffusion and the actual distance covered will depend on the amount of chemical available for diffusion and the stoichiometry of the bleaching reaction. If one makes reasonable assumptions for the chemical demand of pulp, and the size and concentration of bleaching chemical remaining in the segregated regions, penetration distances into the suspension can be estimated. For typical bleaching conditions this distance (to the point of complete chemical consumption) is small, only a fraction of a millimeter (Bennington, 1996).

Thus, an effective chemical contacting strategy for a pulp bleaching operation is to mix chemical to the fiber scale at a rate faster than the effective bleaching rate. The mixture quality exiting the mixer (and entering the retention tower) must also be of sufficient uniformity to optimize the desired pulp quality parameters. The residence time provided by the retention tower cannot be relied upon to create the degree of uniformity needed in all situations.

20-6.1.3 Mixing Quality. The goal of pulp bleaching is to have each fiber react with the appropriate quantity of bleaching chemical. The typical bleaching response with chemical application is nonlinear, as shown in Figure 20-15*b*. Here, the effectiveness of delignification drops off after application of 0.5 to 0.8% ClO_2 on pulp. Chemical application in excess of this amount is not only wasted but permits strength damaging reactions to occur. Thus, an appropriate bleaching strategy must optimize the applied chemical charge.

When mixing is less than perfect, local clumps of fiber see a range of chemical application. Consequently, some fiber will be overtreated and some undertreated. The extent of the effect will depend on the degree of nonuniformity remaining in the suspension and the nature of the bleaching response curve. Homogenization must also be attained faster than the effective chemical reaction rate; otherwise, the degree of nonuniformity during contacting will also affect the bleaching outcome.

20-6.2 Mixing Equipment in Pulp Bleaching Objectives

Mixer design is dictated primarily by the rheology of the suspension, which in turn is largely determined by suspension mass concentration. Thus, certain mixers find predominant use in low, medium, or high consistency bleaching applications. Mixer technology has changed over the years. Certain mixers, such as the stirred tank, are no longer used for pulp bleaching. Other mixers have been developed in response to implementation of new bleaching technologies (e.g., medium consistency ozone bleaching). Descriptions of many mixers used in bleaching applications may be found in Perkins and Doane (1979) and Bennington (1996). A summary of important operational parameters for pulp mixers is given in Table 20-4.

Table 20-4 Characterization of Mixers Used in Pulping Applications

Mixer	Suspension Concentration, C_m	Residence Time (s)	Power Dissipation (MW/m^3)	Energy Expenditure (MJ/t)
Laboratory mixing/mixers				
Hand mixing (bag bleaching)	0.03	180	0.02	120
	0.10	180	0.05	90
High-shear	0.05	10	0.45	63
	0.10	10	1.1–1.8	160–180
Hobart	0.28	30–240	0.08	11–86
Fluffer	0.25–0.40	40–200	0.12–0.16	50–20
Industrial mixers				
Low consistency				
Agitated vessel	0.02–0.04	150–400	0.0002–0.0006	5–9
Static	0.02–0.03	3–5	0.03	4
High-shear/high intensity	0.03–0.04	0.008–1	1–110	3–61
Medium consistency				
Static	0.10	4	0.1	4
Peg	0.10–0.12	10–12	0.08–0.11	11–15
High-shear/high intensity	0.08–0.16	0.025–4	1–110	2–43
Medium consistency pump	0.08–0.11	0.3–0.5	4–5	13–18
Valve and pipe expansion	0.08–0.11	0.3–0.5	1–3	9–11
High consistency				
Schredder type	0.20–0.50	NM[a]	30–70	22–90
Kneader type	0.25–0.45	NM[a]	86–170	70–700

[a] NM, not measured.

20-6.2.1 Low Consistency Applications **($C_m < 0.05$)**. At low mass concentrations, the yield stress is relatively low and abundant free water exists in suspension. Creating motion is relatively easy and is accomplished routinely with agitators for mining stock from high density towers and for consistency control ahead of bleaching. In the past, stirred/agitated reactors of various designs were used for chemical contacting, but experience showed that increased energy dissipation (achieved at the expense of mixer residence time) improved bleaching and reduced chemical use (see Section 20-6.1.1). Although older mixers can still be found in many mill installations, modern practice is to use either static or higher intensity dynamic mixers in these applications.

Static mixers come in a wide range of designs, and a typical one is shown in Figure 20-17. The internal flow elements must allow unimpeded pulp passage to prevent fiber entrapment and plugging while providing mixing action. Residence times are on the order of seconds, but mixing in the axial direction is minimal. Thus, flow of chemical and pulp to the mixer must be uniform. Energy dissipation is approximately 0.03 MW/m^3 (calculated from the pressure drop across the mixer) and is provided by an external stock pump. Care must be taken to ensure that the mixer will provide the required mixing over the anticipated

Figure 20-17 Static mixer used in pulp suspension mixing applications. Shown is the Komax steam mixer used in medium consistency applications.

production range of the plant (turn down), which may fall to as low as 40 to 50% of the normal operating capacity. A typical installation will see two or three static mixers in series, particularly if more than one chemical is used in a bleaching stage. Dynamic high-shear mixers have also been used in low consistency applications. While the energy dissipation is high, the residence time is short, which necessitates precise control of both pulp and chemical flow to the mixer.

20-6.2.2 Medium Consistency Applications **($0.08 \leq C_m \leq 0.16$)**. Many methods have been used to mix chemicals into medium consistency pulp stock. One common approach is to make use of existing equipment to provide the needed chemical contacting. For example, for adjustment of suspension pH before a bleaching stage, one common method is to apply caustic solution across the width of the preceding washer drum discharge (often, >7 m wide) using a shower bar. The pulp is then discharged into a conveyor system and passes through a steam mixer before the bleaching chemical is added. The mixing obtained (through predistribution of chemical and its subsequent agitation in the conveyor and steam mixer) is usually sufficient for slow or nonreacting chemicals.

For rapidly reacting chemicals, turbulence generated in other process equipment can be utilized for mixing. Often, the energy dissipation is similar to that in a dedicated mixer and can be sufficient to disperse flocs. Medium consistency pumps subject pulp to turbulence in the pump approach, in the pump discharge,

and across the flow control valve (Francis and Kerekes, 1992). Liquid chemicals (e.g., chlorine dioxide and hydrogen peroxide) can be added ahead of the pump or directly into the pump suction. For gas applications, sintered metal spargers can be used following the pump but before the flow control valve. Although many mills use these methods, the lack of a dedicated mixer can result in inconsistent mixing. For example, turbulence created across a discharge valve will vary depending on the valve opening (a function of valve position and production rate). Often, a dedicated mixer will improve mixing.

Dedicated medium consistency mixers include peg-type mixers (Figure 20-18*a*). Mixer residence times are around 10 to 12 s with energy dissipation typically about 0.1 MW/m^3. This energy dissipation is insufficient to disrupt individual fiber flocs; rather, pulp is broken into fiber clumps by the mixing action. Chemical is added ahead of or inside the mixer. Multiple injection ports are common for both chemical and steam mixing applications.

High-shear or high intensity mixers are commonly specified for medium consistency applications where the essential design criterion is disruption of fiber flocs during contacting with the bleaching chemical. This requires imposition of sufficient shear, which is often accomplished by creating turbulence within the suspension. Consequently, providing sufficient energy to "fluidize" the suspension is a common design criterion. The flow of pulp and chemical to the mixing zone must be uniform because the suspension rapidly reflocculates upon exiting the high-shear/turbulence zone of the mixer. This can be difficult to achieve, particularly as little backmixing occurs in these mixers. Residence times are typically less than 1 s, and the residence time in the high-shear mixing zone may be only a fraction of this time. A number of high intensity mixers are available, some of which are shown in Figure 20-18(*b*–*e*).

The installation of these high intensity/high-shear mixers in the early 1980s significantly improved chemical utilization in bleaching operations. However, the high power requirements needed by these mixers prompted development of high-shear mixers requiring less attached power. Since the energy dissipation required to create turbulence in the pulp suspension is fixed, power savings were obtained by reducing mixer volume (at the expense of mixer residence time). While one mixer was often adequate in a given bleaching application, two were often used or required.

Most mixer design has been accomplished using pilot trials and in-mill refinements that have resulted in generations of similar mixers having slightly different internals (location and method of chemical addition, rotor configuration, etc.). Recently, computational fluid dynamics has been used to help refine the design of one high-shear mixer. The original mill installation showed significant nonuniformity following the mixer (inferred from the nonuniform temperature profile measured around the pipe circumference at the mixer discharge). A commercial CFD code (Fluent) was used to model the existing mixer, which predicted the nonuniformity observed in the field (Figure 20-19). The model was then used to refine the mixer design to improve chemical distribution. Design changes included

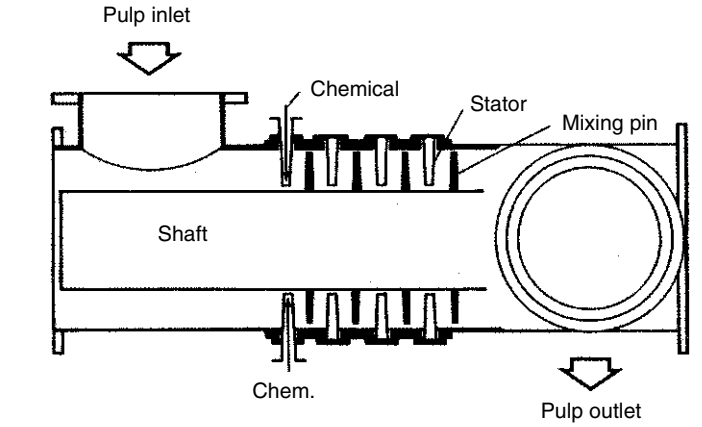

(*a*)

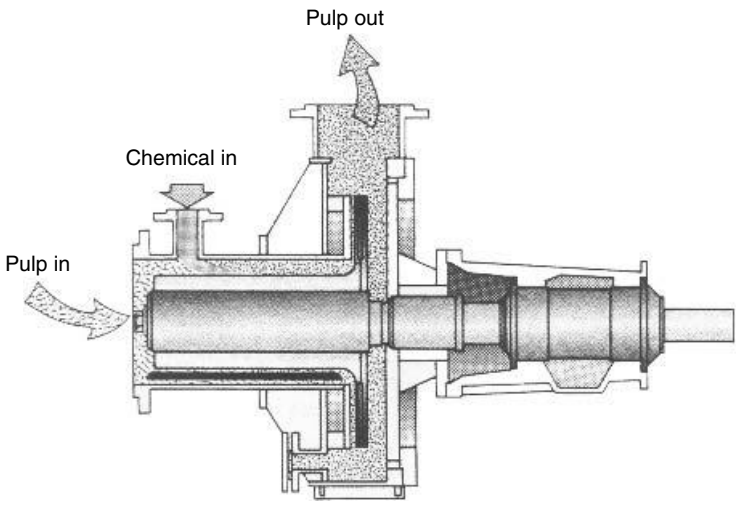

(*b*)

Figure 20-18 Mixers used in medium consistency bleaching applications: (*a*) Beloit peg-type mixer; (*b*) Kamyr high-shear mixer (the first MC fluidizing mixer). (*Continued*)

enlargement of the predistribution vanes at the mixer entrance and use of an involute housing for the mixer chamber. These modifications were implemented in later mixer releases.

Gas mixing presents some unique challenges to mixer designers. For oxygen delignification applications, the typical oxygen volume needed could reach 20 to 30% of the total suspension volume. Rotary mixers tend to separate (de-mix) gas from the suspension. In addition, gas can be held up within the mixer, increasing the effective gas volume of the suspension and reducing the power applied to the suspension. This reduces gas–liquid mass transfer to the suspension. While many

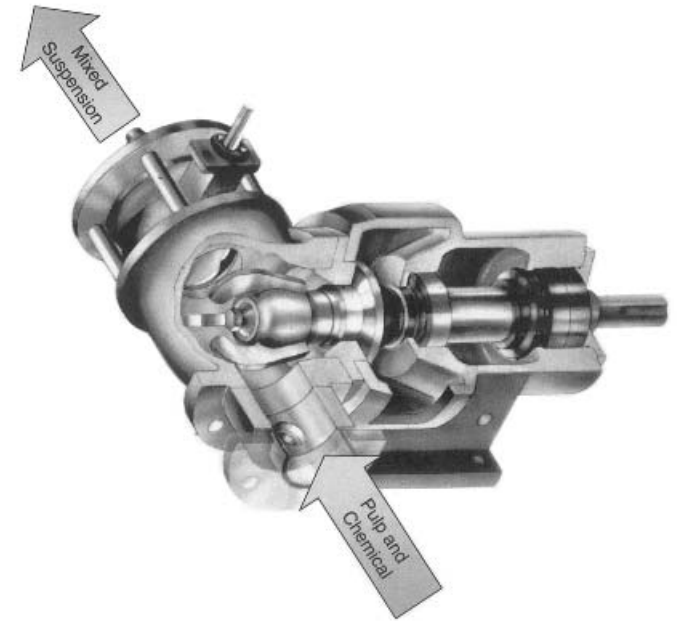

(*c*)

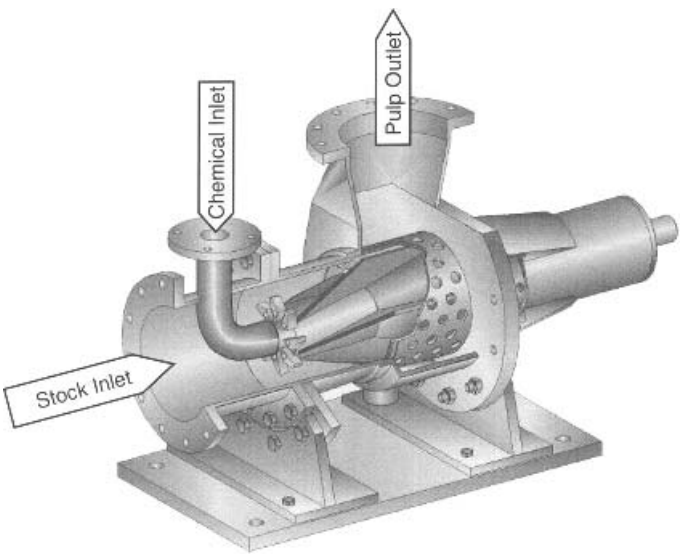

(*d*)

Figure 20-18 (*c*) Ahlmix (Ahlstrom); (*d*) Tri-phase mixer (GL&V).

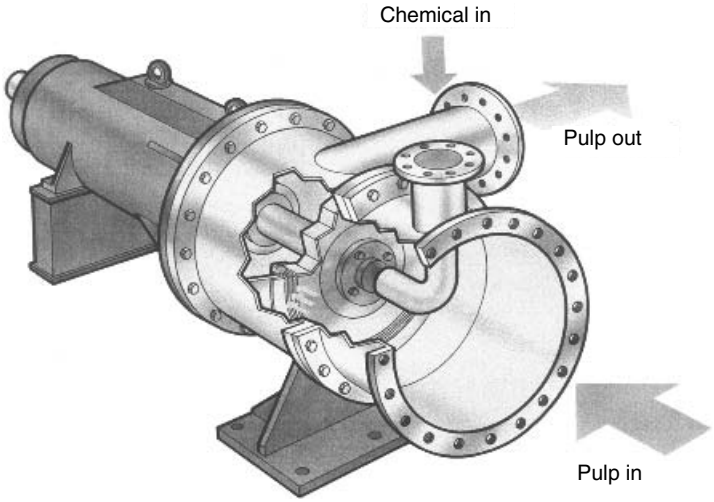

(*e*)

Figure 20-18 (*e*) Sunds MC mixer.

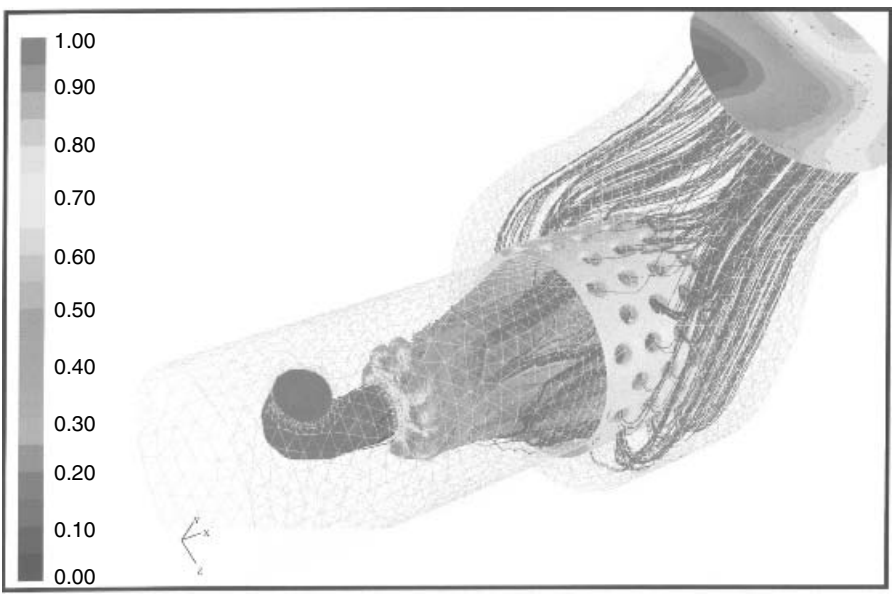

Figure 20-19 CFD solution for flow in an early tri-phase mixer (GL&V) prior to design modifications. Note the spatial distribution of chemical (chlorine dioxide) in the pipe exiting the mixer. See insert for a color representation of this figure.

mixer manufacturers claim that their mixers were capable of handling gas void fractions up to 30% (Greenwood and Szopinski, 1992; Henricson, 1993; Miller et al., 1993), no operating data are published in the open literature. Frequently, mills operating at lower void fractions achieved better system performance.

The gassed power curve for a laboratory mixer operating in water and in a pulp suspension at mass concentrations up to $C_m = 0.16$ is given in Figure 20-20. While a high power draw was maintained in water up to a void fraction of $\phi_g = 40\%$, the power drawn for medium consistency pulp suspensions was reduced to 50% at a void fraction of only 10 to 13%. This is attributed to the yield stress of the suspension that inhibits flow back into the impeller region. Mixing and mass transfer are reduced with reduced power input, and the steep slope of the gassed power curve indicates that any variation in the gas content could dramatically affect the mixing achieved. Indeed, for this mixer design, a minor increase in gas content above 15% could prevent suspension motion entirely (Bennington, 1993; Smith and Bennington, 1995).

The efficiency of industrial high-shear mixers in gas mixing applications has not been measured directly. Despite this, the effectiveness of oxygen delignification processes (which rely on effective oxygen–pulp contacting) has been improved dramatically by implementing process changes designed to minimize gas volume during mixing (Bennington and Pineault, 1999). The magnitude of the improvements realized (delignification efficiencies were increased by 10 to 30 percentage points, more than doubling delignification in some cases) indicates the importance of mixing in these applications.

Medium consistency ozone delignification is practiced in only a limited number of mills worldwide (van Lierop et al., 1996). The amount of ozone required, plus the fact that it is generated at only 7 to 14 wt% in oxygen, means that gas volume fractions of 30% or greater are possible. Existing medium consistency

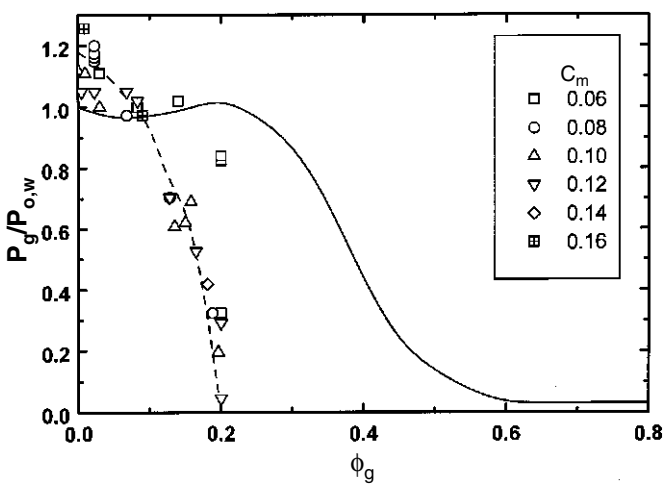

Figure 20-20 Gassed power curve for laboratory pulp mixer (Quantum MK-IV).

mixers could not operate at these high gas contents. One manufacturer (Ahlstrom) designed a mixer to operate under these conditions. Here the flow within the mixer ensures continued gas-suspension contact to maximize the gassed power draw. Power dissipation in the suspension using these mixers is high, reaching 6.5 MW/m^3 for a treatment of 61 MJ/t pulp at void fractions close to 30%.

20-6.2.3 High Consistency Applications **($C_m > 0.20$)**. At high mass concentrations, little or no free water is present in suspension. The mixing strategy used is to expose as much damp fiber surface to chemical as possible. In high consistency oxygen delignification systems, fiber is "fluffed" to generate the fiber surface area using aggressive mixers designed to disrupt the high consistency flocs. These mixers are similar to refiners (see the plate pattern of the A.B. Nilsen mixer in Figure 20-21*a*) and apply tremendous power to the suspension. Chemical can be added during mixing (usually, for liquids), or the fluffed suspension can be transferred to a tower were contact with a gaseous chemical (e.g., oxygen) can be maintained.

Ozone delignification can also be achieved in a high consistency operation. Here, intimate contact with fiber must be achieved quickly. The Union Camp Corp. developed (White et al., 1993) a mixer/contactor based on a peg mixer design to create a dispersion of high consistency fiber in the gas phase (Figure 20-21*b*). Again, the goal was to create fiber surface area. Ozonation proceeds through a shrinking core process (Bennington et al., 1999). Fibers that are not exposed to ozone are not bleached. For liquid mixing, kneader-type mixers can be used. These squeeze the suspension to transfer liquid between regions in the suspension. Again, the high consistency of the suspension necessitates expenditure of considerable energy during the mixing process.

20-6.2.4 Overview of Mixer Characteristics. The wide range of mixers used in pulp bleaching applications can be characterized using a number of parameters. The residence time determines the extent of exposure to mixing action and places an upper limit on the macroscale mixing that might be achieved. The power dissipated during mixing determines if the suspension will be mixed under turbulent conditions, and if floc disruption is likely. Finally, the energy treatment gives an indication of the extent of mixing achieved in a given application. Table 20-4 summarizes these parameters for laboratory mixers (used for bench scale bleaching studies) and for a range of industrial mixers. Although these parameters are indicative of overall mixing performance, they do not account for the different efficiencies often observed between mixers. A number of observations can be made based on these data.

The first observation is that energy expenditure increases with suspension mass concentration. At low consistency, energy expenditure is typically 4 MJ/t. At medium consistency, this varies between 4 and 40 MJ/t. Although it is expected that mixing quality will improve with increased energy treatment, about 10 MJ/t is used by a wide range of mixers that achieve fluidization. For high consistency mixers, energy treatment rises significantly. The rate of mixing can be estimated

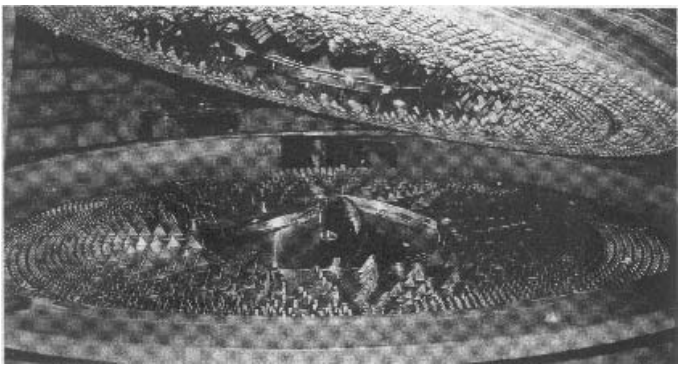

(*a*)

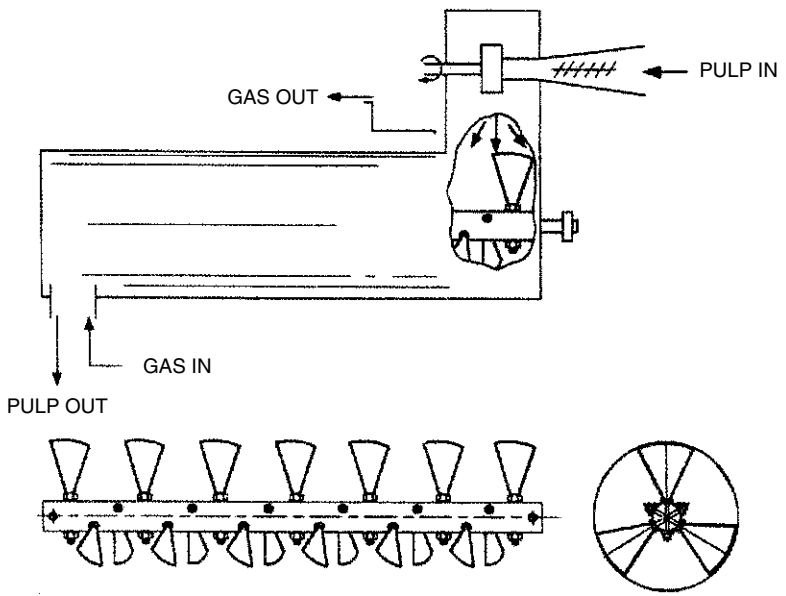

(*b*)

Figure 20-21 Mixers used for high consistency bleaching applications: (*a*) Plate pattern of high consistency mixer (A.B. Nilsen); (*b*) Union Camp ozone mixer/reactor (White et al., 1993).

by the power dissipation per unit volume. In a given application, a mixer having a greater power will be more able to shear flocs apart and achieve a higher rate of fiber scale mixing.

In the past, laboratory bleaching was often represented as an ideal unlikely to be duplicated in the mill. This was based on pulp bleaching using slower-reacting, liquid-based bleaching chemicals mixed by hand. Here, the total energy treatment is typically an order of magnitude greater in the laboratory than in the

mill (120 MJ/t versus 4 to 15 MJ/t). In the mill, low consistency bleaching was accomplished using agitated vessels or static mixers. Medium consistency mixing was largely accomplished using peg-type mixers. Mill adoption of medium consistency technologies (the high-shear/high intensity mixers) saw much higher mixing rates (power dissipation) as well as improved fiber scale mixing (floc dispersion). Mill results could now be as good or better than hand-mixed laboratory results. The mixing dependence of laboratory tests is particularly evident in reactions involving gases, where gas–liquid mass transfer is critical. Transferring laboratory results to the mill is even more difficult here.

20-6.2.5 Incidental Mechanical Action Imparted during Mixing. Mixing consumes energy and results in physical treatment of the pulp fiber. This can alter the physical properties of the pulp. For example, increased energy treatment reduces pulp drainage rate, increases bulk and opacity (for chemical pulps), increases tensile strength, and reduces tear strength. It is common to beat (mechanically refine) pulp to develop its strength properties prior to paper manufacture. Beating reduces tear strength and develops tensile strength, and a balance is sought between these two strength properties by the appropriate application of energy. Additional energy treatment during pulp production may alter the usual delivered pulp properties and affect its perceived strength.

In laboratory bleaching, energy treatment can be significantly higher than that experienced in an industrial setting. Consequently, pulp properties can be significantly different than achieved in the mill, and caution should be exercised when predicting certain pulp properties from these studies. In the mill, the addition of a single medium consistency mixer to a process would only add 3 to 30 MJ/t energy treatment to the pulp. The expected development in strength properties would be too small to be measured. The addition of six to eight of these units (to a bleaching sequence, for example) might increase fiber treatment by up to 200 MJ/t. This would change pulp strength properties by 5 to 10% and may be detectable. In any case, the intrinsic fiber strength, as measured by the zero-span tensile strength, is unaffected by the mechanical treatment (Bennington and Seth, 1989; Seth et al., 1993). Studies made by Bennington and Seth (1998) also showed that there was no synergistic degradation in pulp strength when intense mechanical mixing was applied during ozone bleaching.

20-6.3 Mixing Assessment in Pulp Suspensions

Mixing quality must be quantified to assess its impact on processes and products. Appropriate measurement techniques depend on a number of factors. For mill applications, the technique must not interfere with the process or change pulp properties in any way. More latitude is available for laboratory or pilot scale mixing assessment, although the presence of fibers complicates mixing measurement and assessment. Most mixing assessment techniques are tedious and time consuming to perform.

A number of indices can be used to quantify mixing in pulp suspensions. The coefficient of variation has been used by many investigators (Kolmodin, 1984;

Bergnor et al., 1985; Breed, 1985; Kuoppamaki, 1985; Bennington et al., 1997b) and a mixing index based on it, M, is given by

$$M_x = \frac{\sigma_x}{\bar{x}} \tag{20-37}$$

where x is the measured property (usually, a tracer concentration). M is an appropriate mixing index as Gaussian residual chemical distributions have been measured following mixing (Bennington, 1996). The evaluation scale should also be specified, as M can vary with the assessment scale, as shown in Figure 20-22 (Bennington et al., 1997b).

Other indices can be used to quantify mixing quality. These include the charge deviation (Torregrossa, 1983), which assumes a rectangular distribution of chemical on pulp, and the intensity of segregation, I_S (Paterson and Kerekes, 1985), which is analogous to the turbulent intensity. I_S approaches M for large sample sizes, n ($M = \sqrt{n - 1/n}\, I_S$). In comparisons made in this chapter, $n = 50$, and M and I_S can be considered equivalent. Other investigators (Atkinson and Partridge, 1966; Bennington et al., 2001) have used pulp quality parameters to quantify changes in mixing quality. These methods measure the result of mixing quality (the effect on some measured pulp property, i.e., kappa number, brightness, strength, etc.) rather than mixing uniformity directly.

20-6.3.1 Laboratory Techniques. Mixing assessment at the laboratory and pilot scale have been made using pulp quality parameters and tracer distributions

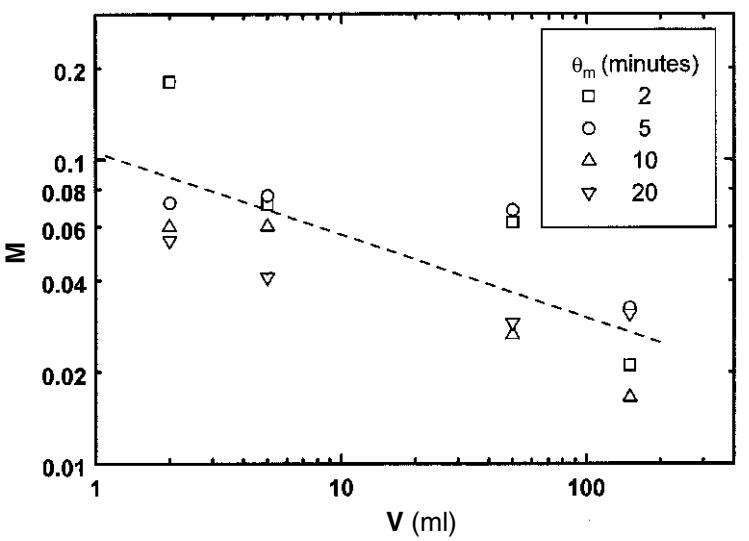

Figure 20-22 Mixing quality, M, as a function of sample volume. Helical pulper (the mixer pictured in figure 20-13) with 8 L of softwood pulp ($C_m = 0.10$) operated at $N = 6.7$ rps. LiCl was used as the tracer. (From Bennington et al., 1997b.)

following mixing. A number of tracers have been used, including inert tracers (those that do not interfere with the pulp) (Breed, 1985; Bennington et al., 1997b; Kamal and Bennington, 2000), dyes (Francis and Kerekes, 1990), and radioactive tracers (Kuoppamaki et al. 1992; Kuoppamaki, 1985). These studies have confirmed that mixing quality measurably affects pulp properties and bleaching efficiency, that achieving uniformity becomes more difficult with increasing suspension mass concentration, and that mixing quality improves as the energy expended in mixing increases. Pilot tests have been used to optimize the location of chemical injection to a mixer (Breed, 1985) and confirm that the point of chemical addition is critical for attaining uniformity. Laboratory tests have also demonstrated the difficulties involved with assessing mixing in pulp suspensions. Suspension sampling is difficult, the quantification tests tedious, and the ability to obtain reproducible measurements problematic. It is common for the 95% confidence interval of a given mixing assessment to be ± 30 to 60% of the measured value (Bennington et al., 1997b).

Predicting the effect of mixing on industrial scale bleaching can be difficult. Often, the pulp quality/economics predicted in the laboratory are difficult to attain in the mill. This leads to the notion that laboratory mixing is "ideal" and that mills that attain process results identical to those in the lab have achieved as good mixing as possible. Recent laboratory work has demonstrated the importance of mixing in certain bleaching stages. Tests measured the efficiency of oxygen delignification using a laboratory high-shear mixer and various mixing strategies (Berry et al., 2002). The extent of delignification varied widely. Delignification ranged from a low of 29% to a high of 50%, depending on both the intensity and duration of mixing. Similar results were found for ozone bleaching (Hurst, 1993) and are likely to occur in other bleaching chemistries. This raises the question: How do we scale-down industrial mixing so that we can use laboratory data to predict industrial performance reliably?

A further problem is the difference between spatial- and mass-based mixing assessments when made on the fiber scale. The distribution of tracer or a residual chemical through a suspension gives a spatial measure of mixing quality. It can be related to pulp quality only if the corresponding mass distribution is known. This is usually not known. Paterson and Kerekes (1986) measured scales of segregation from 2 to 4 mm in their mixing tests—the size of flocs within the suspension. How much does the measured mixing quality depend on the flocculated nature of the suspension, and how much on the distribution of chemical? Fortunately, when mixing is evaluated at scales greater than 5 to 10 cm^3, this problem does not arise because the mass distribution can be considered uniform at this scale.

20-6.3.2 In-mill Mixing Assessment. Mixing assessment in mill operations must be done in a manner that does not upset the process or compromise pulp quality. Past techniques have used mixing quality indices (i.e., pulp brightness, kappa number, etc.) (Atkinson and Partridge, 1966; Elliott and Farr, 1973; Abercrombie, 1986; Cameron, 1987), residual chemical profiles (Paterson and

Kerekes, 1986), inert tracers (Backlund et al., 1987; Robitaille, 1987), and temperature profiling (Torregrossa, 1983; Sinn, 1984; Robitaille, 1987; Rewatkar et al., 2001). Most measurements have been made on the macroscale (scales > 100 cm^3), although Paterson and Kerekes (1986) measured mixing quality on a fiber scale. The assessment techniques used are typically tedious, which limits the amount of data that can be collected. The suspension must also be sampled in a manner that avoids further mixing, which can often be difficult. The use of mixing quality indices requires that pulp samples be bleached in the laboratory for comparison with mill pulps.

The results of reported in-mill studies are included in Tables 20-5 and 20-6. The data show that mixing quality can vary substantially, regardless of the mixer used. Indeed, a given mixer will often perform differently in different mills or in different applications. Mixing quality also varies with process and operating conditions, although the time required to measure mixing has precluded most investigators from acquiring extensive sets of data. Paterson and Kerekes (1986) demonstrated this variability in one mill, where mixing quality was measured in 25 separate tests over a number of days. Even for ostensibly similar operating conditions, the fiber scale mixing quality varied significantly, from $M \simeq I_s =$ 0.00 to 0.30. The time interval between tests was too long (and varied) for the fluctuation frequencies to be identified. An online method of measuring mixing is needed to investigate this issue further.

Often, it is desirable to estimate mixing quality quickly. A common technique used for this purpose is temperature profiling. When a sufficient flow of a cold chemical stream is added to a sufficiently hot pulp stream (as in the D_1 stage), the spatial and temporal variation in temperature following mixing can be interpreted in terms of mixing quality. The assessment of mixing quality is qualitative (only

Table 20-5 Fiber Scale Evaluation of Mixing Quality

Mixer	Mill or Lab	Suspension Mass Concentration, C_m	Tracer/ Technique Used	Sample Volume (cm^3)	Mixing Index, M or I_s	Reference
CST	M	0.03–0.04	Res. Cl^-	7×10^{-8}	0.00–0.51	Paterson and Kerekes (1986)
	L	0.01	LiCl and	0.0005–0.5	0.08–0.14	Kamal and Bennington
	L	0.02	2-NSA	0.0005–0.5	0.04–0.31	(2000)
Static	M	0.025	Res. Cl^-	7×10^{-8}	0.0–0.11	Paterson and Kerekes (1986)
Valve	L	0.082	Dye	Floc	0.14–0.25	Francis and Kerekes (1992)
Hobart mixer	L	0.28	Dye	Floc	0.48–1.15	Francis and Kerekes (1990)
Frotopulper	L	0.26–0.27	Dye	Floc	0.27–0.45	Francis and Kerekes (1990)
High shear	L	>0.25	LiCl	Floc	0.10–0.13	Turnbull (private communication)

Table 20-6 Macroscale Evaluation of Mixing Quality

Mixer	Mill or Lab	Suspension Mass Concentration, C_m	Tracer/ Technique Used	Sample Volume (cm^3)	Mixing Index, M	Reference
Tower	M	0.095–0.12	LiCl	50	0.26–0.50	Kolmodin (1984)
	M	0.089–0.122	LiCl	200	0.14–0.74	Bergnor et al. (1985)
	M	0.108	LiCl	Handful	0.40	Torregrossa (1983)
Repulper	L	0.03	LiCl	50	0.008	Bennington et al. (1997b)
	L	0.08	LiCl	50	0.008	
	L	0.08	LiCl	2	0.05	
Static	M	Low	Ba-137	64	0.12	Kuoppamaki (1985)
	M	0.13?	LiCl	Handful	0.40–0.60	Torregrossa (1983)
	M	Low	Ba-137	15 000	0.005	Kuoppamaki (1985)
Peg	M	0.106	LiCl	Handful	0.20–0.40	Torregrossa (1983)
High shear	L	0.10	LiCl	2	0.03	Bennington et al. (1997b)
	L	0.10	LiCL	5	0.02	
	M	0.095–0.12	LiCl	50	0.02–0.05	Kolmodin (1984)
	M	0.10	LiCl	200	0.06–0.08	Bergnor et al. (1985)
	L	0.11–0.13	LiCl	300–400	0.06–0.53	Breed (1985)
	M	0.106	LiCl	Handful	0.05–0.10	Torregrossa (1983)
	L	0.09–0.11	Ba-137	~500 (axial)	<0.05	Kuoppamaki et al. (1992)
	M	0.08–0.11	Temp	~1400 (axial)	0.10–0.40	Rewatkar et al. (2001)

the circumferential suspension temperature is measured, and temperature-based mixing indices do not allow estimation of potential chemical savings directly). Quantitative estimates can be made by making mass and energy balances on the added chemical (Rewatkar et al., 2001).

An example of temperature profiling is given in Figure 20-23. In a mill bleach plant, an older-style peg mixer used for chlorine dioxide mixing in the D_1 stage was replaced with a high-shear dynamic mixer to improve mixing quality. Following mixer replacement, chemical use unexpectedly increased 2.0 kg/t (18%). A series of thermograms taken of the process piping immediately following the new chlorine dioxide mixer showed that the cold chlorine dioxide stream channeled through the mixer. The temperature difference between the lower and upper sides of the pipe was 12°C. As the medium consistency pulp flowed as a plug after exiting the mixer, there was little dispersion or further mixing of the suspension. In this case, mixing was improved by changing the method of chemical addition ahead of the mixer. Following the modifications, chemical use decreased by 3.5 kg ClO_2/t, a savings of 1.5 kg ClO_2/t over the original peg mixer installation. This illustrates that mixing cannot be taken for granted—newer mixers do not necessarily guarantee better mixing.

Temperature profiling can also be used to examine variability in mixing quality with time (Rewatkar et al., 2001). As shown in Figure 20-24, the mixing index (based on the variability in measured temperature around the pipe circumference) changed significantly before and after the impeller. Following the mixer, mixing

Figure 20-23 Thermograph of exit piping following a high-shear chlorine dioxide mixer in D_1 service. Elbow immediately following mixer discharge. The temperature is 12°C higher along the top of the pipe. See insert for a color representation of this figure.

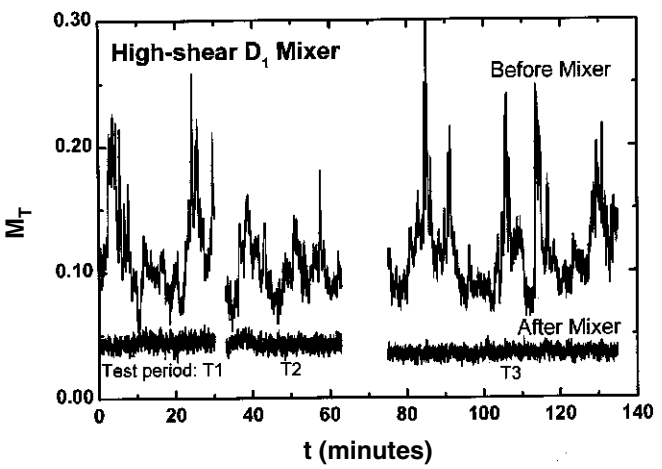

Figure 20-24 Mixing index based on temperature variation (M_T) versus time for a high-shear chlorine dioxide mixer in D_1 service. Mixing quality is evaluated following chemical injection both before and following mixing.

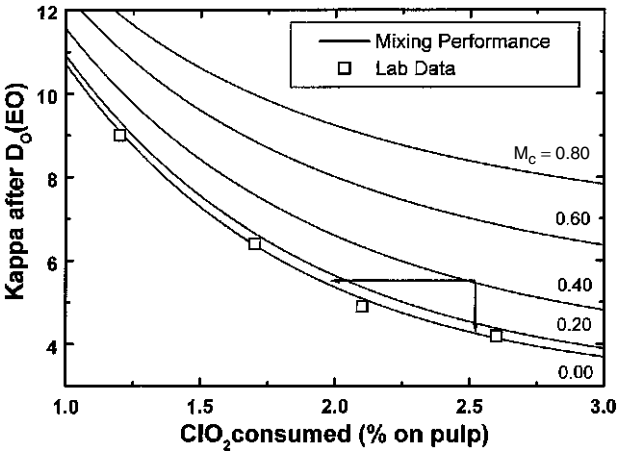

Figure 20-25 Mixing performance curves generated for a softwood pulp having an initial kappa number of 27.6. Pulp was laboratory bleached using a D(EO) partial sequence. (Reaction conditions were: D: T = 48°C for 30 min at $C_m = 0.035$ to an end pH of 1.9 to 2.5; EO: T = 70°C for 60 min at $C_m = 0.10$ to an end pH of 11.5).

quality is improved and constant. Mass and energy balances can be used to convert the temperature-based index measured in Figure 20-24 to a chemical charge-based index that is more representative of system performance. For the D_1 mixer assessed in Figure 20-24, this would be M = 0.33, indicating that chemical savings are possible (see Figure 20-25).

20-6.4 Benefits of Improved Mixing

The benefits of improved mixing have been known for a long time. Following the introduction of medium consistency mixer technology in the 1980s, a CPPA survey documented chemical savings averaging 10 to 15% (Berry, 1990). Mills that took advantage of the improved mixing technology saw their capital investment returned in as little as three months. The situation is no different in mills today, and significant chemical savings can be achieved through improved mixing. However, mixing quality must be measured to know the degree to which it can be improved.

The chemical savings potential is readily demonstrated in Figure 20-25. Here, the mixing performance curves for a kraft pulp delignified using a D_0(EO) sequence (a chlorine dioxide stage followed by extractive oxidation stage) are given. The curve for "perfect" mixing (M = 0.0) was determined in the laboratory under "ideal" mixing conditions. The other curves were calculated with these data assuming a normal distribution of chemical throughout the suspension following mixing. The mixing index is defined using eq. (20-37). To illustrate the benefits of improved mixing, assume that an existing mixer achieves a mixing quality of M = 0.40 (which is typical of many installations; see Tables 20-5

and 20-6) and the process operates at the point indicated in the figure. Here an average chemical charge of 2.5% is needed to reduce the kappa number from 27.6 to 5.5. Improving mixing quality to $M = 0.05$ would allow the process to be moved anywhere on the corresponding performance curve (Note that the $M = 0.05$ curve is almost equivalent to the $M = 0.0$ curve.) This gives an engineer a number of options. He or she can choose to minimize chemical use in the D_0 stage, achieving the same exit kappa number using a chemical charge of only 1.6%. For a 1000 t/day mill, this would save about $1.4 million (Canadian) annually in chemical. Alternatively, the engineer can maintain the chemical charge and go into the subsequent bleaching stage at a lower kappa number. This is often the strategy of choice where the efficiency of a process using an inexpensive bleaching chemical is improved. Oxygen delignification is a good example. Here improved mixing has increased delignification efficiencies from 30% to the range 40 to 55+%. Chemical savings would be minimal in the oxygen stage (as oxygen is inexpensive), but by reducing the kappa number entering the Do stage, chemical savings in chlorine dioxide of up to $3 to $5 per metric ton could be achieved (Bennington and Pineault, 1999). This is equivalent to approximately 5 to 10% the bleaching cost of pulp. A combination of these strategies allows optimization of the overall bleaching sequence.

Improved mixing offers other benefits. Pulp strength and brightness ceilings can be improved, which would have beneficial marketing implications. In addition, synergism with other processes can be achieved, in particular, with process control systems used throughout the mill.

20-7 CONCLUSIONS

Mixing is a critical unit operation in many pulp and paper operations. A wide range of mixing strategies are employed throughout the industry. Some of these applications are common in other industries and are detailed in other chapters of this book. Some mixing applications are unique to pulp and paper production, particularly those involving pulp fiber suspensions. In either case, mixing affects the efficiency of many processes, directly and synergistically. Attaining optimal mixing conditions can improve product quality and reduce costs.

NOMENCLATURE

a, b	parameters
a	particle dimension (m)
A	fiber aspect ratio, l_w/d
B	number of rotor vanes
C_I	effective ink concentration (ppm)
C_m	fiber mass concentration (as a fraction, unless specified otherwise)
C_R	contact area between fiber and suspension (m^2)
C_v	fiber volume concentration (as a fraction, unless specified otherwise)

d	fiber diameter (m)
D	diffusion rate (m^2/s)
D	impeller/rotor diameter (m)
D_m	mean impeller/rotor diameter (m)
F	Tappi flake content, fraction
F_R	force applied per unit length of rotor (N/m)
G	rotor swept area (m^2/rev)
H_C	height of rotor in contact with suspension (m)
I_S	intensity of segregation
k_{eff}	effective first-order reaction rate (s^{-1})
k, k_0	rate of deflaking (m^{-2})
k_I	rate of ink detachment (s^{-1})
k_La	volumetric gas–liquid mass transfer coefficient (s^{-1})
k_R	rate of ink redeposition (s^{-1})
K	proportionality constant
l_w	length-weighted fiber length (m)
L	length of cylindrical rotor (m)
m	stock parameter [eq. (20-23)] (m/s)
m_i	mass of component i (kg)
M_x	mixing index of x [see eq. (20-37)]
n	sample size
N	rotor speed (rps)
P	impeller power (W)
r_a	cavern radius (m)
S	rotor swept area (m^2)
t	time (s)
T	temperature (°C)
T	vessel diameter (m)
T	shaft torque ($N \cdot m$)
T_M	material strength (wet tensile strength) (N/m)
x	measured variable
X_w	mass of water absorbed per mass of fiber material (kg/kg)

Greek Symbols

α	constant determined by geometry and extent of diffusion
γ	shear rate (s^{-1})
ε	energy dissipation (W/kg)
ε_{avg}	average energy dissipation measured in the liquid phase, per unit mass (W/kg)
ε_{in}	energy input per unit mass (W/kg)
ε_{loc}	local energy dissipation measured in the liquid phase, per unit mass (W/kg)
ε_v	energy dissipation per unit volume (W/m^3)
ε_F	energy dissipation per unit volume at the point of fluidization (transition to turbulence) (W/m^3)

μ_a	apparent viscosity (Pa · s)
μ_p	plastic viscosity (Pa · s)
ν	kinematic viscosity (m^2/s)
ρ_i	density of component i (kg/m^3)
σ_x	standard deviation of variable x
τ_y	yield stress (Pa)
τ_E	micromixing time constant (s)
τ_M	mixing time constant (s)
τ_D	diffusion time constant (s)
τ_R	reaction time constant (s)
ϕ_i	volume fraction of component i

Subscripts

f	fiber
g	gas
w	water

Superscripts

0	initial
f	floor level

REFERENCES

Abercrombie, D. A. (1986). C_D and D_1 high intensity mixers reduce bleaching costs at Westar, *Proc. CPPA Spring Conference, Pacific Coast and Western Branches*, Jasper, Alberta, Canada, May 14–17.

Atkinson, E. S., and H. de V. Partridge (1966). Effects of mixing and degree of chlorination on quality and bleaching costs, *Tappi J.*, **49**(2), 66A–72A.

Backlund, B., E. Bergnor, P. Sandstom, and A. Teder (1987). The benefits of better mixing, *Pulp Paper Can.*, **88**(8), T279–T285.

Bakker, A., and J. B. Fasano (1993). A computational study of the flow pattern in an industrial paper pulp chest with a side entering impeller, in *Process Mixing: Chemical and Biochemical Applications*, Part II, G. B. Tatterson, R. V. Calibrese, and W. R. Penny, eds., *AIChE Symp. Ser.*, **293**(89), 118–124.

Baldyga, J., and J. R. Bourne (1989). Simplification of micromixing calculations: I. Derivation and application of new model, *Chem. Eng. J.*, **42**, 83–89.

Baldyga, J., and J. R. Bourne (1999). *Turbulent Mixing and Chemical Reactions*, Wiley, Chichester, West Sussex, England.

Ben, Y., and G. Dorris (1999). Irreversible ink deposition during repulping: II. ONP/OMG furnishes, *Proc. 5th Research Forum on Recycling*, PAPTAC, Ottawa, Ontario, Canada, Sept. 28–30, pp. 7–13.

Bennington, C. P. J. (1988). Mixing pulp suspensions, Ph.D. dissertation, University of British Columbia, Vancouver, British Columbia, Canada.

Bennington, C. P. J. (1993). Mixing gases into medium-consistency pulp suspensions using rotary devices, *Tappi J.*, **76**(7), 77–86.

Bennington, C. P. J. (1996). Mixing and mixers, in *Pulp Bleaching: Principles and Practice*, C. W. Dence and D. W. Reeve, eds., Tappi Press, Atlanta, GA, pp. 537–568.

Bennington, C. P. J. (1999). *Understanding defibering and ink detachment during repulping*, in *Paper Recycling Challenge*, Vol. III, *Process Technology*, M. R. Doshi and J. M. Dyer, eds., Doshi & Associates, Appleton, WI, pp. 268–282.

Bennington, C. P. J., and J. R. Bourne (1990). Effect of suspended fibres on macromixing and micro-mixing in a stirred tank reactor, *Chem. Eng. Commun.*, **92**, 183–197.

Bennington, C. P. J., and R. J. Kerekes (1996). Power requirements for pulp fluidization, *Tappi J.*, **79**(2), 253–258.

Bennington, C. P. J., and J. P. Mmbaga (1996). The use of mixing-sensitive chemical reactions for the study of mixing in pulp fiber suspensions, in *Mixed Flow Hydrodynamics: Advances in Engineering Fluid Mechanics*, N. P. Cheremisinoff, ed., Gulf Publishing, Houston, TX.

Bennington, C. P. J., and J. P. Mmbaga (2001). Fluid phase turbulence in pulp fibre suspensions, *Trans. 12th Fundamental Research Symposium*, Oxford, C. F. Baker, ed., Pulp and Paper Fundamental Research Society, Vol. 1, pp. 255–286.

Bennington, C. P. J., and I. Pineault (1999). Mass transfer in oxygen delignification systems: mill survey results, analysis and interpretation, *Pulp Paper Can.*, **100**(12), T395–T403 (123–131).

Bennington, C. P. J., and R. S. Seth (1989). Response of pulp fibres to mechanical treatment during MC fluidization, *Trans. 9th Fundamental Research Symposium*, Cambridge, Mechanical Engineering Publications, London, Vol. 1, pp. 87–103.

Bennington, C. P. J., and R. S. Seth (1998). Pulp strength and incidental mechanical treatment during kraft pulp bleaching, *Proc. International Pulp Bleaching Conference*, Helsinki, Finland, June 1–5, Book 1, pp. 167–173.

Bennington, C. P. J., and V. K. Thangavel (1993). The use of a mixing-sensitive chemical reaction for the study of pulp fibre suspension mixing, *Can. J. Chem. Eng.*, **71**, 667–675.

Bennington C. P. J., and M.-H. Wang (2001). A kinetic model of ink detachment in the repulper, *J. Pulp Paper Sci.*, **27**(10), 347–352.

Bennington, C. P. J., R. J. Kerekes, and J. R. Grace (1989). Mixing in pulp bleaching, *J. Pulp Paper Sci.*, **15**(5), J186–J195.

Bennington, C. P. J., R. J. Kerekes, and J. R. Grace (1990). The yield stress of fibre suspensions, *Can. J. Chem. Eng.*, **68**, 748–757.

Bennington, C. P. J., R. J. Kerekes, and J. R. Grace (1991). Motion of pulp fibre suspensions in rotary devices, *Can. J. Chem. Eng.*, **69**, 251–258.

Bennington, C. P. J., G. Azevedo, D. A. John, S. M. Birt, and B. H. Wolgast (1995). The yield-stress of medium- and high-consistency pulp fibre suspensions at high gas contents, *J. Pulp Paper. Sci.*, **21**(4), J111–J118.

Bennington, C. P. J., G. Owusu, and D. W. Francis (1997a). Gas–liquid mass transfer in pulp suspension mixing operations, *Can. J. Chem. Eng.*, **75**, 53–61.

Bennington, C. P. J., C. M. Peters, and R. MacLaren (1997b). Characterization of mixing quality in laboratory pulp mixers, *J. Pulp Paper Sci.*, **23**(9), J459–J465.

Bennington, C. P. J., O. S. Sui, and J. D. Smith (1998a). The effect of mechanical action on waste paper defibering and ink removal in repulping operations, *J. Pulp Paper Sci.*, **24**(11), 341–348.

Bennington, C. P. J., J. D. Smith, O. S. Sui, and M. -W. Wang (1998b). Characterization of repulper operation for newsprint deinking, *Proc. Tappi Pulping Conference*, Montreal, Quebec, Canada, Oct. 25–29, pp. 1083–1095.

Bennington, C. P. J., X. -Z. Zhang, and A. R. P. van Heiningen (1999). Effect of fibre-width distribution on ozone bleaching, *J. Pulp Paper Sci.*, **35**(4), 124–129.

Bennington, C. P. J., H. T. Yang, and G. Pageau (2001). Mill assessment of mixing quality using laboratory bleaching studies, *Pulp Paper Can.*, **102**(11), T305–T309.

Bergnor, E., B. Backlund, and A. Teder (1985). The Benefits of Better Mixing, *Proc. International Pulp Bleaching Conference*, Quebec, Canada, TAPPI/CPPA, pp. 233–241.

Berry, R. (1990). High-intensity mixers in chlorination and chlorine dioxide stages: survey results and evaluation, *Pulp Paper Can.*, **91**(4), T151–T159.

Berry, R., Z. H. Jiang, M. Faubert, B. van Lierop, and G. Sacciadis (2002). Recommendations from computer modelling for improving single stage oxygen delignification systems, *Proc. PAPTAC Annual Technical Conference*, Montreal, Quebec, Canada, pp. B151–B161.

Bialkowski, W. L. (1992). Newsprint variability and its impact on competitive position, *Pulp Paper Can.*, **93**(11), T299–T306.

Biermann, C. J. (1996). *Handbook of Pulping and Papermaking*, 2nd ed., Academic Press, San Diego, CA.

Blasinski, H., and E. Rzyski (1972). Mixing of non-Newtonian liquids: 2. Power consumption for fibrous suspensions, *Inzh. Chem.*, **2**(1), 169–182.

Bouchard, J., V. Magnotta, and R. Berry (2000). Improving oxygen delignification with peroxymonosulfate: the (OPx) process, *Proc. International Pulp Bleaching Conference*, Halifax, Nova Scotia, Canada, oral presentations, pp. 97–113.

Breed, D. B. (1985). Discovering the mechanisms of pulp mixing: a pilot approach to high shear mixing, *Proc. Medium Consistency Mixing Seminar*, Hollywood, FL, Nov. 7–8, Tappi Press, Atlanta, GA, pp. 33–37.

Cameron, M. (1987). Sunds high intensity mixer performance on C_D and D_1 Stages, *Proc. CPPA Spring Conference, Pacific Coast and Western Branches*, Whistler, British Columbia, Canada, May 14–16.

Dence, C. W., and D. W. Reeve (1996). *Pulp Bleaching: Principles and Practice*, Tappi Press, Atlanta, GA.

Dobson, H. A. (2001). The mixing sensitivity of polysulfide generation, M.A.Sc. thesis, University of British Columbia, Vancouver, British Columbia, Canada.

Dobson, H. A., and C. P. J. Bennington (2002). The mixing sensitivity of polysulfide generation, *Can. J. Chem. Eng.*, **80**(2), 214–223.

Dorris, G. M. (2000). Effects of impeller type and mixing power on settling and filtering of lime mud, *J. Pulp Paper Sci.*, **26**(2), 47–53.

Dorris, G. M., and V. C. Uloth (1994). Analysis of oxidized white liquors: II. Potentiometric titrations for the determination of polysulfides and sulphoxy anions, *J. Pulp Paper Sci.*, **20**(9), J242–J248.

Dosch, J. B., K. M. Singh, and T. J. Stenuf (1986). Air content of medium and high consistency pulp slurries, *Proc. Tappi Engineering Conference*, Atlanta, GA, pp. 721–723.

Ein Mozaffari, F., G. A. Dumont, and C. P. J. Bennington (2001). Performance and design of agitated stock chests, *Pacwest Conference, Pulp and Paper Technical Association of Canada*, Whistler, British Columbia, Canada, May 16–19.

Elliott, R. G., and T. D. Farr (1973). Mill-scale evaluation of chlorine mixing, *Tappi J.*, **56**(11), 68–70.

FAO (1999). *Recovered Paper Data, 1997–1998*, Food and Agriculture Organization of the United Nations, Rome.

Francis, D. W., and R. J. Kerekes (1990). Measurement of mixing in high-consistency pulp suspensions, *J. Pulp Paper Sci.*, **16**(4), J130–J135.

Francis, D. W., and R. J. Kerekes (1992). Flow and mixing behaviour of low-consistency and medium-consistency fiber suspensions downstream of a valve, *Tappi J.*, **75**, 113–119.

Frederick, W. J., Jr., R. Krishnan, and R. J. Ayers (1990). Prissonite deposits in green liquor processing, *Tappi J.*, **72**(2), 135–140.

Gibbon, J. D., and D. Attwood (1962). The prediction of power requirements in the agitation of fibre suspensions, *Trans. Inst. Chem. Eng.*, **40**, 75–82.

Grace, T. M., and E. W. Malcolm, eds. (1989). *Pulp and Paper Manufacture*, Vol. 5, Alkaline Pulping Joint Textbook Committee, CPPA/TAPPI, Montreal, Quebec, Canada and Atlanta, GA.

Greenwood, B. F., and R. Szopinski (1992). Ozone Bleaching Technology '92, *Proc. Non-chlorine Bleaching Conference*, Miller Freeman, San Francisco.

Gullichsen, J., and C. J. Fogelholm, eds. (1999). *Chemical Pulping*, Books 6A and 6B, Fapet Oy, Helsinki, Finland.

Gullichsen, J., and E. Harkonen (1981). Medium consistency technology: I. Fundamental data, *Tappi J.*, **64**(6), 69–72.

Henricson, K. (1993). Modern bleaching technology, *Proc. Non-chlorine Bleaching Conference*, Miller Freeman, San Francisco.

Holman, K. L., R. P. Warrick, J. D. Farrelly, and T. D. McDonald, Jr. (1989). Analysis of mixing in a smelt dissolver, *Proc. Tappi Pulping Conference*, Seattle, WA, pp. 761–768.

Hurst, M. M. (1993). Effects of pulp consistency and mixing intensity on ozone bleaching, *Tappi J.*, **76**(4), 156–161.

Jang, H. F., and R. S. Seth (1998). Using confocal microscopy to characterize the collapse behaviour of fibers, *Tappi J.*, **81**(5), 167–174.

Jansson, I., ed. (1999). *Accurate Consistency: A Handbook on Accurate Consistency Measurement in Pulp and Paper Processing*, BTG Pulp and Paper Technology, Saffe, Sweden.

Kamal, N. R., and C. P. J. Bennington (2000). An on-line, in-situ, mixing assessment technique for pulp fibre suspensions, *J. Pulp Paper Sci.*, **26**(6), 214–220.

Kerekes, R. J., R. M. Soszynski, and P. A. Tam Doo (1985). The flocculation of pulp fibres, in *Trans. 8th Fundamental Research Symposium*, Oxford, V. Putnam, ed., Fundamental Research Committee, Oxford, Vol. 1, pp. 265–310.

Kolmodin, H. (1984). How to save costs by mixing chlorine dioxide and pulp homogeneously, *Svensk Papperstid.*, **87**(18), 8–14.

Kuoppamaki, R. (1985). The quality of mixing studied using a radiotracer technique, in *Medium Consistency Mixing Seminar*, Hollywood, FL, Nov. 7–8, Tappi Press, Atlanta, GA, pp. 13–17.

Kuoppamaki, R., O. Pikka, and K. Peltonen (1992). New high-intensity MC® mixer: direct measurement of mixing efficiency, *Proc. European Pulp and Paper Week, New Available Techniques and Current Trends*, SPCI/ATICELCA, Bologna, Italy, May 19–22, pp. 216–224.

Ljungqvist, M., and H. Theliander (1995). Mixing conditions in the smelt dissolver, *Proc. International Chemical Recovery Conference*, Toronto, Ontario, Canada, April 24–25, CPPA/TAPPI, pp. A283–A289.

Makinen, M. (1999). Coating color preparation, in *Pigment Coating and Surface Sizing of Paper*, E. Lehtinen, ed., Book 11 in the series Papermaking Science and Technology, Fapet Oy, Helsinki, Finland, pp. 319–388.

Mann, R. (1983). *Gas–Liquid Contacting in Mixing Vessels*, Institution of Chemical Engineers, Rugby, Warwickshire, England.

McKinney, R. (1998). Flotation deinking overview, in *Paper Recycling Challenge*, Vol. III, *Process Technology*, M. R. Doshi and J. M. Dyer, eds., Doshi & Associates, Appleton, WI, pp. 99–114.

Middleton, S. R., and A. M. Scallan (1993). Partial lumen loading, *Nordic Pulp Paper Res. J.*, **8**(1), 204–207, 231.

Miller, B., L. D. Shackford, and S. Minami (1993). Oxygen, peroxide and ozone process equipment, *Proc. Non-chlorine Bleaching Conference*, Miller Freeman, San Francisco.

Mmbaga, J. P. (1999). The use of mixing-sensitive chemical reactions to characterize mixing in the liquid phase of fibre suspensions, Ph.D. dissertation, University of British Columbia, Vancouver, British Columbia, Canada.

Morgan, J. P., and F. E. Murray (1971). Mass transfer and chemical reaction rate considerations in high efficiency black liquor oxidation designs, *Tappi J.*, **54**(9), 1500–1504.

Oldshue, J. Y. (1983). Pulp and paper agitation, in *Fluid Mixing Technology*, McGraw-Hill, New York.

Paterson, A. H. J., and R. J. Kerekes (1984). Fundamentals of mixing in pulp suspensions: diffusion of reacting chlorine, *Tappi J.*, **67**(5), 114–117.

Paterson, A. H. J., and R. J. Kerekes (1985). Fundamentals of mixing in pulp suspensions: measurement of microscale mixing of chlorine, *J. Pulp Paper Sci.*, **11**(4), J108–J113.

Paterson, A. H. J., and R. J. Kerekes (1986). Fundamentals of mixing pulp suspensions: measurement of microscale mixing in mill chlorination mixers, *J. Pulp Paper Sci.*, **12**(3), J78–J83.

Perkins, J. K., and F. P. Doane, Jr. (1979). Pulp bleaching equipment, in *The Bleaching of Pulp*, R. P. Singh, ed., Tappi Press, Atlanta, GA.

Pulp and Paper International (2001). *World's Pulp, Paper Board Ind. Prod. Trade*, **43**(7); 8–9.

Reeve, D. W., and A. B. McKague (1990). Identification of chlorinated compounds in bleached pulp extracts, *EUCEPA 24th Conference Proc.*, Stockholm, Sweden, May 8–11, pp. 468–478.

Rewatkar, V. B., and C. P. J. Bennington (2000). Gas–liquid mass transfer in low- and medium-consistency pulp suspensions, *Can. J. Chem. Eng.*, **78**, 504–512.

Rewatkar, V. B., R. J. Kerekes, and C. P. J. Bennington (2001). The use of temperature profiling to measure mixing quality in pulp bleaching operations, *Proc. Annual Technical Meeting, PAPTAC*, Montreal, Quebec, Canada, pp. B135–B143.

Reynolds, E., J. D. Gibbon, and D. Attwood (1964). Smoothing quality variations in storage chests holding paper stock, *Trans. Inst. Chem. Eng.*, **42**, T13–T21.

Robinson, J. V., N. Millman and J. B. Whitley (1997). The dispersion of pigments for paper coating, Chapter 3 in *Pigments for Paper*, R. Hagemeyer, ed., Tappi Press, Atlanta, GA, pp. 21–53.

Robitaille, M. A. (1987). High intensity mixing at the chlorine dioxide stage, *Pulp Paper Can.*, **88**(4), T109–T111.

Rydholm, S. A. (1965). *Pulping Processes*, Wiley-Interscience, New York.

Scallan, A. M., and J. E. Carles (1972). The correlation of the water retention value with the fibre saturation point, *Svensk Papperstid.*, **75**, 699–703.

Seth, R. S., D. W. Francis, and C. P. J. Bennington (1993). The effect of mechanical treatment during medium stock concentration fluidization on pulp properties, *Appita*, **46**(1), 54–58.

Shaharuzzaman, M., and C. P. J. Bennington (2001). The effect of mixing on the generation of alkaline peroxymonosulfate, *Can J. Chem. Eng.*, **79**(4), 595–601.

Shaw, I. S. D., and R. D. Christie (1984). Low cost and energy efficient oxidizer (ECO), *Pulp Paper Can.*, **85**(3), T40–T43.

Sinn, S. (1984). State-of-the-art chlorine dioxide mixer installed at Weyerhaeuser, *Pulp Paper*, June, pp. 119–121.

Smith, R. J., and C. P. J. Bennington (1995). Mixing gases and pulp suspensions in a continuous laboratory mixer, *Appita*, **48**(6), 414–418.

Smook, G. A. (1992). *Handbook for Pulp and Paper Technologists*, 2nd ed., Angus Wilde Publishing, Vancouver, British Columbia, Canada.

Soloman, R., T. P. Elson, A. W. Nienow, and G. W. Pace (1981). Cavern sizes in agitated fluids with a yield stress, *Chem. Eng. Commun.*, **11**, 143–164.

Somasundaran, P. and L. Zhang (1998). *Fundamentals of flotation deinking*, in *Paper Recycling Challenge*, Vol. III, *Process Technology*, M. R. Doshi and J. M. Dyer, eds., Doshi & Associates, Appleton, WI, pp. 83–98.

Tatterson, G. B. (1991). *Fluid Mixing and Gas Dispersion in Agitated Tanks*, McGraw-Hill, New York.

Tessier, P., and M. Savoie (1997). Chlorine dioxide delignification kinetics and Eop extraction of softwood kraft pulp, *Can. J. Chem. Eng.*, **75**, 23–30.

Thibault, F. (1999). Analyse du procede de melange solide-liquide: application a la préparation des sauces de couchage du papier, Ph.D. dissertation, Université de Montreal, Montreal, Quebec, Canada.

Thring, R. W., V. W. Uloth, G. M. Dorris, T. S. Galvin, D. Hornsey, and J. R. Ayton (1995). White liquor oxidation in a pilot plant pipeline reactor, *Tappi J.*, **78**(1), 107–113.

Torregrossa, L. O. (1983). Effect of mixing efficiency on chlorine dioxide bleaching, *Proc. Tappi Pulping Conference*, Houston, TX, Oct. 24–26, pp. 635–641.

Uloth, V., G. Dorris, R. Thring, R. Hogikyan, J. Wearing, L. Tench and J. Ayton (1996). In situ production of polysulfide liquor in a kraft mill's causticizers, *Proc. Tappi Pulping Conference*, Tappi Press, Atlanta, GA, pp. 813–836.

Van Lierop, B., A. Skothos, and N. Liebergott (1996). Ozone delignification, in *Pulp Bleaching: Principles and Practice*, C. W. Dence and D. W. Reeve, eds., Tappi Press, Atlanta, GA, p. 335.

Walker, O. J., and A. Cholette (1958). Determination of the optimum size and efficiency of stock chests: I. The ideal chest, *Pulp Paper Can.*, Mar., pp. 113–117.

White, D. E., T. P. Gandek, M. A. Pikullin, and W. H. Friend (1993). Importance of reactor design in high-consistency ozone bleaching, *Pulp Paper Can.*, **94**(9), T242–T247.

Yackel, D. C. (1998). *Pulp and Paper Agitation: The History, Mechanics and Process*, Tappi Press, Atlanta, GA.